

AN ASSESSMENT OF FIN-TUBE THERMAL CONTACT RESISTANCE IN  
ROUND-TUBE-PLAIN-FIN HEAT EXCHANGERS

BY

MARIA CORTES

THESIS

Submitted in partial fulfillment of the requirements  
for the degree of Master of Science in Mechanical Engineering  
in the Graduate College of the  
University of Illinois at Urbana-Champaign, 2015

Urbana, Illinois

Adviser:

Professor Anthony M. Jacobi

## ABSTRACT

Fin-and-tube heat exchangers are used in a wide variety of applications. Heat exchangers with expanded tubes are economical, but a drawback is the potentially large contact resistance between tubes and fins. Previous studies have investigated this topic under the exclusion of air-side convection. The present work is more realistic, because the contact resistance is evaluated in the presence of air-side convection. The goal of this experimental work is to determine the contribution of the contact resistance to the overall heat transfer resistance in round-tube-plain-fin heat exchangers. The four samples have copper tubes with two different expansion ratios and aluminum fins with collars of two different lengths. The heat exchangers were examined in a wind tunnel under dry and frosted conditions to determine the contact resistance. The frosted heat exchangers are used as a baseline, because frost growth bridges the gaps between fins and tubes. The contact resistance was much higher for the unexpanded heat exchangers – about 30-60% of the overall resistance, whereas expanded heat exchangers exhibited a contact resistance of about 10-30% of the overall resistance.

## ACKNOWLEDGMENTS

I would like to thank my advisor Professor Anthony Jacobi for his guidance and support throughout this project. I am also grateful to the members of the Air Conditioning and Refrigeration Center for their advice. For their encouragement and support, I especially owe thanks to Jessica Bock and my husband David Cortes.

# Table of Contents

List of Figures .....	v
List of Tables .....	vi
List of Symbols .....	vii
Chapter 1 – Introduction .....	1
1.1 Background .....	1
1.2 Literature Review.....	2
Chapter 2 – Experimental Methods .....	5
2.1 Experimental Setup.....	5
2.2 Experimental Procedure.....	6
2.3 Data Reduction.....	7
2.4 Figures .....	11
2.5 Tables.....	12
Chapter 3 – Results and Discussion.....	14
3.1 Temperature dependence .....	14
3.2 Contact Resistance .....	16
3.3 Figures .....	17
3.4 Tables.....	21
Chapter 4 – Conclusion.....	23
References.....	24
Appendix A – Uncertainty Analysis .....	26
Appendix B – Data Processing .....	29
Appendix C – Calibrations.....	31
Appendix D – Data .....	41

## List of Figures

Figure 1. Schematic of heat exchanger, indicating height (H), width (W), and flow depth/length (L) .....	11
Figure 2. Top view of two heat exchangers with different fin spacing. Top: 591 FPM. Bottom: 394 FPM.....	11
Figure 3. Closed-loop wind tunnel. (1 - pre-heaters, 2 - cool-mist humidifier, 3 - pre-cooler, 4 - after heaters, 5 - blower, 6 - mixing chamber, 7 - contraction, 8 - test section, 9 - hot wire velocity measurement, 10 - static mixer) .....	12
Figure 4: Resistance model for fin-and-tube heat exchangers with fin collars.....	12
Figure 5: Temperature dependence of resistance for a unit surface area for different Reynolds numbers.....	17
Figure 6: Heat exchanger 2 at time of minimum resistance with frost starting to build up between fins at the top.....	18
Figure 7: Heat exchanger 3 with excessive frost buildup from the sides .....	18
Figure 8: Resistances for unit surface area under dry and frosted conditions and calculated contact resistance .....	19
Figure 9: Contact resistance in percent of overall resistance.....	20
Figure 10: Contact resistance for unit contact area.....	20
Figure 11: Uncertainties of Measured Variables in EES Uncertainty Propagation.....	27
Figure 12: Lookup Table for fluid mass flow rate .....	30
Figure 13: Lookup Table for fluid properties .....	30

## List of Tables

Table 1: Heat exchanger matrix .....	12
Table 2: Features and dimensions of heat exchanger samples .....	13
Table 3: Heat exchanger 1: Resistances and temperature dependence parameters a and b at different Reynolds numbers .....	21
Table 4: Heat exchanger 2: Resistances and temperature dependence parameters a and b at different Reynolds numbers .....	21
Table 5: Heat exchanger 3: Resistances and temperature dependence parameters a and b at different Reynolds numbers .....	21
Table 6: Heat exchanger 4: Resistances and temperature dependence parameters a and b at different Reynolds numbers .....	22
Table 7: Measurement uncertainties .....	26
Table 8: Calibration curves and uncertainty for RTDs .....	31
Table 9: Thermocouple calibration curves and uncertainties for upstream thermocouples ..	31
Table 10: Thermocouple calibration curves and uncertainties for downstream thermocouples ..	32
Table 11: Calibration data for RTDs .....	32
Table 12: Thermocouple calibration data .....	34
Table 13: Data set from heat exchanger 4 .....	41

## List of Symbols

$A$	Area	[m <sup>2</sup> ]
$C$	Heat capacity rate	[W/K]
$c$	Specific heat	[J/kg-K]
$C_R$	Ratio of min. over max. heat capacity rate	[ - ]
$D$	Diameter	[m]
$FPM$	Fins per meter	[ /m ]
$\dot{m}$	Mass flow rate	[kg/s]
$NTU$	Number of transfer units	[ - ]
$T$	Temperature	[K]
$Q$	Heat transfer rate	[W]
$R$	Thermal resistance	[K/W]
$u$	Uncertainty	
$v$	Velocity	[m/s]

## Greek Symbols

$\varepsilon$	Effectiveness	[ - ]
$\Phi$	Weight factor	[ - ]
$\varphi$	Relative humidity	[ % ]

## Subscripts

$air$	Air
$air,in$	Air inlet condition
$air,out$	Air outlet condition

$c$	Contact
$f$	Frontal (area)
$h$	hydraulic (diameter)
$\max$	Maximum
$\min$	Minimum
$r$	Coolant
$r,in$	Coolant inlet condition
$r,out$	Coolant outlet condition
$s$	Surface (area)
$T$	Total

# Chapter 1 – Introduction

Fin-and-tube heat exchangers are commonly used for heat transfer between liquid, steam, or refrigerants in the tubes and air that flows through the fins. They are a type of compact heat exchanger manufactured either by brazing the fins to tubes of the same material, usually aluminum, or by expanding the tubes in the fin stack. This latter method can be performed by mechanical, hydraulic, or pneumatic expansion whereby a bullet or hydraulic or pneumatic pressure forces the tube to expand. For expanded-tube heat exchangers, the tubes and fins do not need to be the same material, commonly the tubes are made of copper and the fins of the more lightweight aluminum.

The mechanical contact between the expanded tubes and the fins or fin collars is not continuous, and small gaps at the interface can have a significant effect on the overall thermal resistance of the heat exchanger. The purpose of this study is to provide an estimate of the impact of contact resistance on performance for typical round-tube-plain-fin heat exchangers under operating conditions typical to air conditioning and refrigeration. In making this assessment, the heat exchangers are subjected to realistic conditions, taking into account convective heat transfer on the air side.

## 1.1 Background

Fin-and-tube heat exchangers with expanded tubes are commonly used for HVAC&R systems. In the common construction, copper tubes are inserted into aluminum fins and then expanded mechanically, hydraulically or pneumatically. Residual stresses from the expansion maintain the contact between tubes and fins. The contact pressure can be controlled, *e.g.* by tool size (bullet size) in a mechanical expansion, but is also influenced by the operating temperature via thermal expansion. As opposed to brazing fins and tubes together, which provides a metallurgical bond, the expansion process results in imperfect mechanical contact that poses a resistance to heat transfer.

The surface waviness and roughness leads to only discrete points on the surfaces being in contact with each other and the rest of the surfaces being separated by a gap. Surface characteristics of fins and tubes (*e.g.* Sheffield, Stafford, & Sauer, 1985) and bond and gap resistances (*e.g.* Gardner & Carnavos, 1960) have been investigated, but for practical purposes an average contact resistance over the whole heat exchanger is of interest. This average contact resistance is important, because it may be a significant part of the overall heat transfer resistance.

## 1.2 Literature Review

Madhusudana *et al.* (1990) reviewed the extant literature 25 years ago and found that research on cylindrical contact areas was scarce. The authors noticed that the contact resistance in finned tubes and fin-and-tube heat exchangers was never directly measured, but calculated from the measured total resistance and an estimate of the other resistances from correlations or other experiments. In most studies, the contact resistance was found to be a small part (<15%) of the overall resistances, especially at lower temperatures.

An influential study by Dart (1959) was motivated by trying to find a non-destructive test for quality assurance. The method is not aimed at determining the contact resistance in absolute terms. The results of the experiments were intended for comparison and quality control and absolute values of contact resistance were not necessarily expected to be reliable. The thermal conductivity between adjacent tubes was measured by alternating hot and cold water flows through neighboring tubes connected by fins. An insulating blanket was wrapped around the heat exchangers in order to eliminate convection. This approach led to a resistance model whereby all resistances from the hot tubes to the cold tubes are in series: convection resistance in the tubes, conduction resistance through the tube walls, contact resistance, and conduction resistance through the fins. This model has been adopted by other researchers who investigated contact resistance, although improvements to the experimental setup were implemented. Dart concluded that thinner fins (0.15 mm in his experiment) require a higher interference to reach the same level of bond conductivity as thicker fins (0.25 mm). Heat exchangers with thicker fins and a high interference could be almost as effective as soldered fins. The overall heat transfer

coefficient of expanded tube heat exchangers with undamaged collars was 10 to 40% lower than that of a heat exchanger with soldered contact areas.

Experiments by Sheffield and colleagues examined several fin-and-tube heat exchangers in a setup similar to Dart's experiment (Sheffield, Abu-Ebid, & Sauer, 1985) (Sheffield, Wood, & Sauer, 1989). The samples were placed in a vacuum in order to eliminate convection on the air side. It was determined that the thermal contact resistance depends on interfacial pressure between tubes and fins. Correlations for the thermal contact conductance, which is the inverse of contact resistance, as a function of fin number, fin thickness, net interference, and tube diameter were presented in both papers. Contact resistance could be as high as 55% of overall resistance. The operating temperature is not a factor in the correlations. Another paper presents a testing technique to determine fin-to-tube bond quality based on axial pull strength of the joint (Ernest, Sheffield, & Sauer, 1985), stressing the importance of contact pressure for thermal contact resistance.

Kim *et al.* examined mechanically expanded fin-and-tube heat exchangers in a vacuum in a series of papers (Kim, Jeong, & Youn, 2003) (Jeong, Kim, Youn, & Kim, 2004) (Jeong, Kim, & Youn, 2006), closely resembling Sheffield's experiments. The authors considered different expansion ratios, fin types, and fin spacings. A numerical procedure was implemented along with the experimental method to predict contact resistance. The numerical model included axial conduction along the tubes, but not convection on the air side. The study found that thermal contact resistance decreases with increasing tube expansion ratio (contact pressure) and decreasing fin spacing. Contact resistance was found to be between 10 and 20% of the overall resistance. The authors acknowledge that the percentage of the contact resistance in the overall resistance might be smaller, if air-side convection was considered. Different temperatures on the hot side were found to have no effect on the resistance.

Gardner and Carnavos (1960) examined finned tubes in a wind tunnel with hot steam on the tube side. Contact resistance was split up into bond and gap resistance. It was found that the bond resistance was relatively small compared to the other resistances. At elevated temperatures, differential thermal expansion between fins and tubes relaxed the contact pressure and increased the gap resistance. The tubes in this study had individual circular fins that expanded away from the tubes at higher temperatures. Gardner and Carnavos developed a theoretical model for

predicting gap resistance from fin and tube dimensions, their physical properties, the fluid temperatures and heat transfer coefficients, and the initial contact pressure. In this model, the different resistances were considered to be in series. In the experimental results, the contact resistance was lumped in with the air-side convection resistance.

Critoph *et al.* (1996) considered wavy-fin-and-tube air-conditioning condensers in two different experiments. The performance of each condenser was measured in a wind tunnel first by supplying electric heat to the tubes, then by circulating R22. After the experiments, the specimens were sectioned and examined under a microscope. The condensers had two rows of mechanically expanded copper tubes in aluminum fins. The study compared these condensers to heat exchangers that were bonded with an aluminum brazing method, but otherwise identical. The contact resistance for these latter heat exchangers was assumed to be negligible, which made the calculation of the contact resistance possible. In this study, the contact resistance was determined to be as high as 12% of the air-side resistance.

ElSherbini *et al.* (2003) examined plain-fin heat exchangers made only from aluminum. The fins had no collars and the tubes were pressed into the fins through slots from the sides. The tubes were expanded pneumatically after insertion. Two heat exchangers were subjected to experiments under dry and frosting conditions; one was as manufactured, the other one was brazed. The unbrazed heat exchanger exhibited a very high contact resistance under dry conditions, which became insignificantly small under frosted conditions. It was concluded that frost bridged the gaps between fins and tubes and practically eliminated the contact resistance. This conclusion was confirmed by comparison to measurements for the brazed heat exchanger. The contact resistance was expressed as a percentage of air-side resistance. Results showed that the contribution of the contact resistance to the air-side resistance was between 82 and 100% of the air-side resistance. The inclusion of air-side convection leads to two parallel paths for heat transfer on the air side, namely by convection from the outer surfaces of the tubes and by conduction across the contact between tubes and fins and then through the fins.

## Chapter 2 – Experimental Methods

Four fin-and-tube heat exchangers with two different values of fin spacing were subjected to experiments. For each fin spacing, there was one heat exchanger with expanded tubes and one with unexpanded tubes (Table 1). The heat exchangers with unexpanded tubes represent the worst case of a poor expansion process, *e.g.* due to worn out tools. A schematic of the heat exchangers is provided in Figure 1, and the dimensions are given in Table 2. The two different values of fin spacing corresponding to 394 and 591 fins per meter (FPM) are illustrated in Figure 2.

As previously shown by ElSherbini *et al.* (2003), an expanded tube heat exchanger exhibits the same resistance in the initial stages of frost growth as a brazed heat exchanger. Frost bridges the gaps between tubes and fins or fin collars and thereby virtually eliminates the contact resistance. Therefore, all four heat exchangers in this study were subjected to experiments with dry- and frosted-surface conditions in order to determine the contact resistance.

### 2.1 Experimental Setup

All four heat exchangers were subjected to experiments in a closed-loop wind tunnel (Figure 3). The blower provided air-side face velocities from 1 m/s to 4 m/s. After passing through a pre-heater, a pre-cooler and a humidifier, the air went through the blower and a mixing chamber. A contraction connects the mixing chamber to the test section which has a cross-sectional area of 15 cm x 15 cm. The air temperature upstream of the test section was measured with an array of 16 T-type thermocouples, calibrated against a NIST-certified precision thermometer, which was itself calibrated to an accuracy of  $\pm 0.003$  K. The combined uncertainty of the upstream thermocouple array was  $\pm 0.049$  K, where uncertainties were combined in accordance with a method presented by Park *et al.* (2010). Similarly, the downstream temperature was measured with 20 thermocouples. The overall uncertainty of this array was  $\pm 0.072$  K. The mixing chamber upstream provided a uniform temperature profile. Downstream of the heat exchanger, a uniform temperature profile was ensured by a static mixer made from

acrylic sheet between the test section and the thermocouple array. The relative humidity was measured upstream of the heat exchanger using a temperature/humidity data logger with an accuracy of  $\pm 2\%$  RH. The air temperature was regulated primarily with a refrigerated bath circulator with a temperature range of -10°C to 100°C and a cooling capacity of 240 W, which was connected to the pre-cooler in the tunnel. An electric pre-heater with a variable power supply was also employed. As a redundant measurement to double check the energy balance for the heat exchanger, the air velocity was measured intermittently with a handheld hot wire anemometer with a measurement uncertainty of  $\pm 0.2$  m/s far downstream of the test section.

An aqueous solution of ethylene glycol (DOWTHERM 4000) with a concentration of 68% EG was used as the tube-side fluid. An external chiller cooled a large reservoir of this solution to the desired temperature. The coolant from the reservoir was circulated through the heat exchanger specimens using a 2.2 kW pump. A flow rate of approximately 0.077 kg/s ( $Re_D = 1000$ ) was maintained. The coolant temperature was measured with two PT100 platinum RTDs close to the inlet and outlet of the heat exchanger. The RTDs were also calibrated with the above precision thermometer to accuracies of  $\pm 0.029$  K and  $\pm 0.025$  K. A Coriolis mass flow meter with an accuracy of  $\pm 1\%$  of the reading was used to determine the mass flow rate of the fluid. A LabVIEW program acquired data every three seconds and stored it in a text file. Data were recorded continuously and data from unsteady conditions were discarded after analysis.

## 2.2 Experimental Procedure

Data were first acquired under dry conditions with all inlet and outlet temperatures above the dew point of the air in the tunnel (0°C to 5°C, depending on ambient conditions). The air temperature was kept steady to within  $\pm 0.1^\circ\text{C}$ . Preliminary experiments showed that the overall resistance to heat transfer varied with the coolant temperature. Therefore, data were acquired for different coolant temperatures above the dew point in order to determine the temperature dependence of the resistance in the absence of condensation or frost formation.

After obtaining data for dry-surface conditions, the coolant temperature was lowered to below the frosting point, to a temperature of -11°C. Upon reaching this temperature, the

humidifier delivered additional moisture for condensation and frosting. The experiment was monitored and the water bath temperature was adjusted to maintain a steady air inlet temperature. As frost formed in the interstitial space at the fin-tube junctions, the overall thermal resistance reached a minimum, the resistance then rose steeply as the frost layer thickened on the fins. At the end of each experiment, the humidifier was turned off and the top of the tunnel was opened in order to let the moisture escape in preparation for the next run.

Each heat exchanger was subjected to experiments at different air mass flow rates and at different air temperatures, which were kept steady during each experiment. The coolant temperature varied by approximately  $0.7^{\circ}\text{C}$  due to the cycles of the chiller. The chiller does not have a variable cooling power, so it chilled the coolant to just below the target temperature and then turned off. The coolant would then slowly warm up again, until the chiller turned back on. The obtained data during the slow warming-up phase were assumed to represent a quasi-steady state, whereas the data from the quick cooling phase do not represent a steady state condition and were discarded.

### 2.3 Data Reduction

An  $\varepsilon$ -NTU method was used to determine the overall resistance. The effectiveness,  $\varepsilon$ , was calculated following a method laid out by Domingos (1969). From the energy balance, the rate of heat transfer can be expressed in terms of the heat capacity rate and the temperature difference of the air stream or the fluid stream (Eqs. 1 and 2).

$$q = C_a (T_{a,in} - T_{a,out}) \quad 1)$$

$$q = C_f (T_{f,out} - T_{f,in}) \quad 2)$$

where

$$C_a = \dot{m}_a c_{p,a} \quad 3)$$

$$C_f = \dot{m}_f c_{p,f} \quad 4)$$

The overall effectiveness  $\varepsilon$  is the ratio of the actual heat transfer  $q$  as calculated with Eq. 2 and the maximum possible heat transfer  $q_{max}$ . Since  $C_a < C_f$ ,  $q_{max}$  is calculated using the air side heat capacity rate, which cancels out and leaves a ratio of temperature differences.

$$\varepsilon = \frac{q}{q_{max}} = \frac{C_a (T_{a,in} - T_{a,out})}{C_a (T_{a,in} - T_{f,in})} = \frac{T_{a,in} - T_{a,out}}{T_{a,in} - T_{f,in}} \quad 5)$$

In order to find the number of transfer units  $NTU$ , and hence the resistance  $R$ , the effectiveness of each individual tube pass  $\varepsilon_{pass}$  is needed. Domingos (1969) introduced a generalized approach for complex heat exchanger assemblies which can be applied to the heat exchangers in this study by dividing them into three heat exchangers in series in an overall counter-flow arrangement, representing the three tube columns. A one-dimensional fin conduction analysis suggests that conduction between these three division can be neglected, since the adiabatic line between the tube columns diverges from the midline by no more than 7%. Each tube column is then subdivided into six passes. The overall effectiveness is a function of the effectiveness of the tube columns (Eq. 6). The effectiveness of each tube column is in turn a function of the effectiveness of each pass (Eq. 8).

$$\varepsilon = \frac{1 - \left( \frac{1 - \varepsilon_{col} C_r}{1 - \varepsilon_{col}} \right)^3}{C_r - \left( \frac{1 - \varepsilon_{col} C_r}{1 - \varepsilon_{col}} \right)^3} \quad 6)$$

where

$$C_r = \frac{C_{min}}{C_{max}} = \frac{(\dot{m}c_p)_a}{(\dot{m}c_p)_f} \quad 7)$$

$$\varepsilon_{col} = \frac{1}{C_r} \left[ 1 - \left( 1 - \frac{C_r \varepsilon_{pass}}{6} \right)^6 \right] \quad 8)$$

Finally the effectiveness of each pass can be expressed as a function of  $NTU$  (Eq. 9) as in Incropera *et al.* (2007), since then it is a simple single-pass cross-flow arrangement with the air side unmixed and the fluid side mixed for each individual tube.

$$\varepsilon_{pass} = \frac{6}{C_r} \left[ 1 - \exp \left\{ -\frac{C_r}{6} [1 - \exp(-NTU_{pass})] \right\} \right] \quad 9)$$

The heat capacity rate of air for the overall and the column effectiveness depends on the total mass flow rate, whereas the heat capacity rate for each individual tube is based on a sixth of the total mass flow rate, assuming that each of the six tubes in each of the three columns receives the same fraction of the overall mass flow rate.

After obtaining the number of transfer units per pass  $NTU_{pass}$ , the resistance to heat transfer of each pass can be calculated from Eq. 10. Here,  $C_{min}$  is divided by six, because each tube only receives a sixth of the air flow.

$$R_{pass} = \frac{1}{NTU_{pass} C_{min}/6} \quad 10)$$

The resistances of the tube passes are in parallel with each other when considering the whole heat exchanger. In analogy to electrical circuits, the overall resistance to heat transfer can be calculated from the individual resistances using Eq. 11.

$$\frac{1}{R_{Total}} = \sum_{i=1}^{18} \frac{1}{R_i} = \frac{18}{R_{pass}} \quad 11)$$

or

$$R_{Total} = \frac{R_{pass}}{18} = \frac{1}{3 NTU_{pass} C_{min}} \quad 11a)$$

Using Domingos' method leads to resistances that are almost identical to those when using an equation given by Incropera *et al.* (2007) (Eq. 12) as an approximation. Here, a crossflow single pass arrangement with mixed fluid and unmixed air is assumed. The overall resistance is then calculated with Eq. 13.

$$NTU_{crossflow} = -\ln \left[ 1 + \frac{1}{C_R} \ln(1 - \varepsilon C_R) \right] \quad 12)$$

$$R_{Total,crossflow} = \frac{1}{C_{min} NTU_{crossflow}} \quad 13)$$

As previously mentioned, a heat exchanger in the initial stages of frosting exhibits the same resistance as a brazed heat exchanger (ElSherbini, Jacobi, & Hrnjak, 2003). The brazed heat exchanger has the same air-side, fin, and tube-side resistances as the expanded one, but the contact resistance is negligible. Since convection on the air side is included in the experiment, there are two parallel paths for heat transfer. One is through convection to the fins and conduction through them, the other one is through convection to the outside of the fin collars (Figure 4). The remaining resistances are in series and are simply added up for the overall resistance (Eq. 14). If the contact resistance changes, the total resistance changes by the same amount. The contact resistance is therefore easily calculated from the difference between the total resistance under dry and under frosted conditions (Eq. 15).

$$R_T = R_{t,conv} + R_{t,cond} + R_c + R_{collar} + \left( \frac{1}{R_{air,conv}} + \frac{1}{R_f} \right)^{-1} \quad 14)$$

$$R_c = R_{T,dry} - R_{T,frost,min} \quad 15)$$

The overall resistance of the heat exchangers in this study was found to vary with the inlet temperature of the coolant, even before frosting. This suggests that thermal expansion plays a role and needs to be accounted for. Experiments showed that the relationship between coolant temperature and resistance is linear in the absence of condensation. Since condensation could only be avoided down to the dew point, the resistance was extrapolated to the temperature at which frosting was conducted. Therefore,

$$R_{Total,dry}(T_{frost}) = a \times T_{frost} + b \quad 16)$$

where  $a$  is the slope of the linear fit and  $b$  the intercept.

## 2.4 Figures

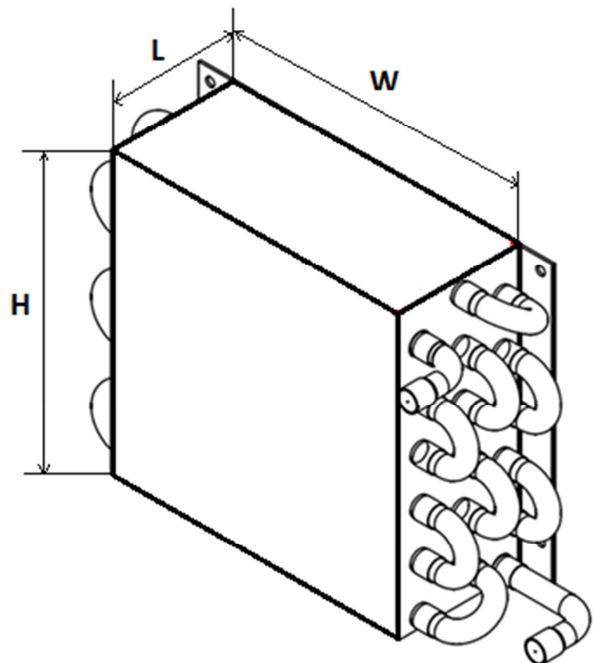


Figure 1. Schematic of heat exchanger, indicating height (**H**), width (**W**), and flow depth/length (**L**)

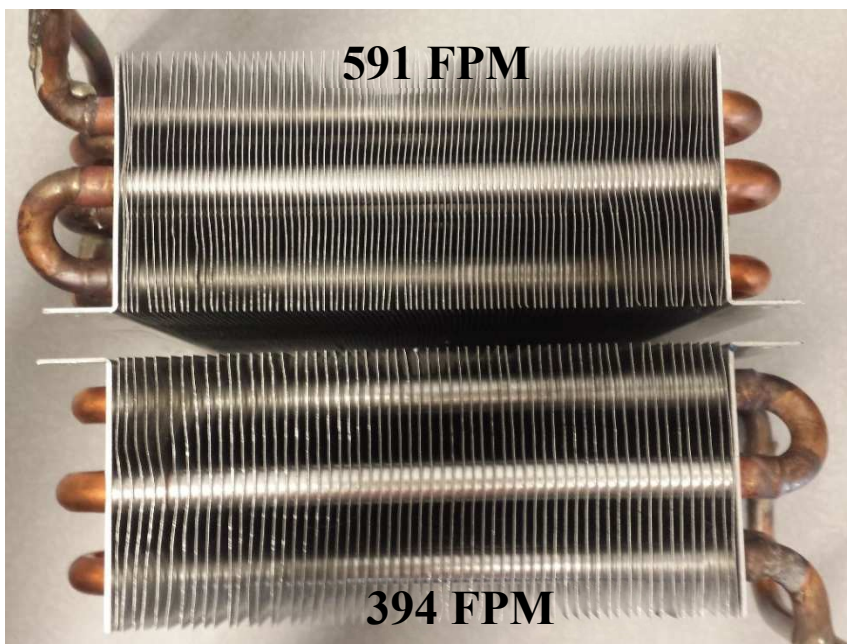


Figure 2. Top view of two heat exchangers with different fin spacing. Top: 591 FPM. Bottom: 394 FPM

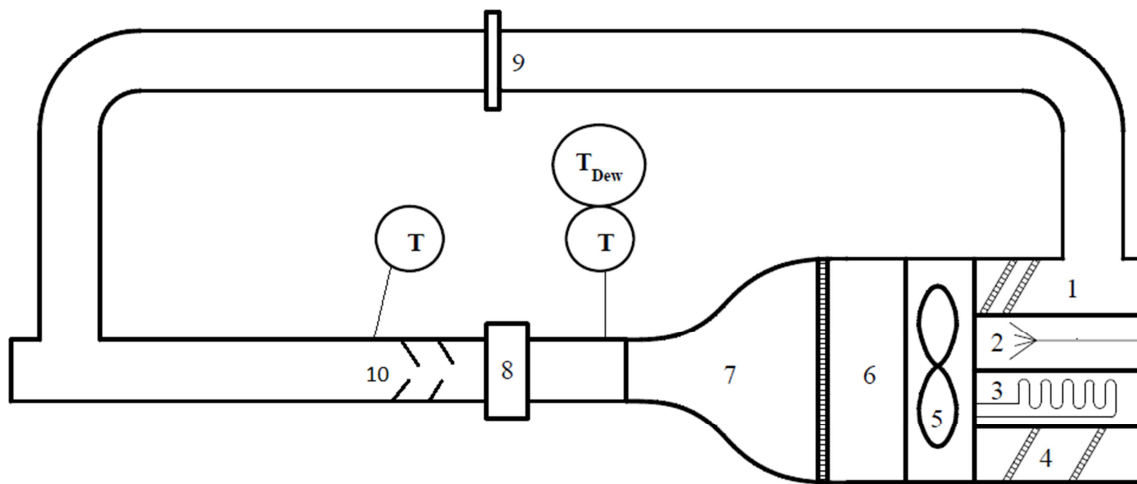


Figure 3. Closed-loop wind tunnel. (1 - pre-heaters, 2 - cool-mist humidifier, 3 - pre-cooler, 4 - after heaters, 5 - blower, 6 - mixing chamber, 7 - contraction, 8 - test section, 9 - hot wire velocity measurement, 10 - static mixer)

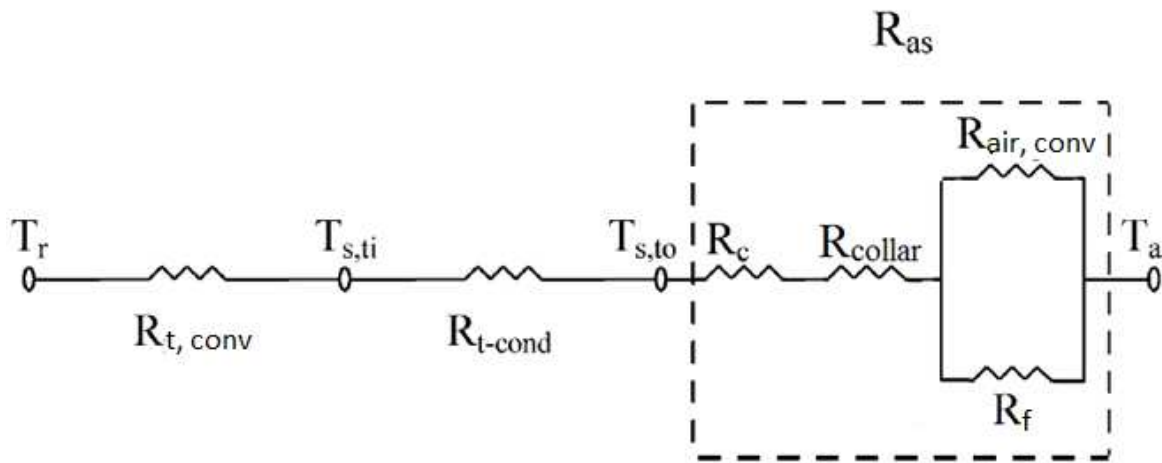


Figure 4: Resistance model for fin-and-tube heat exchangers with fin collars

## 2.5 Tables

Table 1: Heat exchanger matrix

	FPM	Expansion	$A_s (m^2)$	$A_f (m^2)$	$D_h (m)$
HX 1	394	Unexpanded	1.1021	0.0138	0.0033
HX 2	394	Expanded	1.1021	0.0138	0.0033
HX 3	591	Unexpanded	1.6535	0.0126	0.0020
HX 4	591	Expanded	1.6535	0.0126	0.0020

*Table 2: Features and dimensions of heat exchanger samples*

Fin Material	Aluminum
Tube Material	Copper
Width W	15 cm
Length L	6.6 cm
Height H	15 cm
Tube OD	9.5 mm
Tube Thickness	0.4 mm
Fin Thickness	0.19 mm
Fin Spacing	394 or 591 FPM
Number of Tubes	18
Number of Tubes Rows	3

## Chapter 3 – Results and Discussion

### 3.1 Temperature dependence

The temperature dependence of the overall resistance on the coolant temperature was investigated for each heat exchanger sample at different air temperatures and mass flow rates. For all cases, the resistance increased with decreasing coolant inlet temperature. Examples of this dependence for the four heat exchangers are shown in Figure 5.

Previous researchers also saw changes in resistance with inlet temperatures. Gardner and Carnavos (1960) reported for example that tube-side steam temperatures in the range of 100–200°C with air cooling the fin side led to a relaxation of the contact pressure and increased resistance for finned tubes, especially if the air temperature was also elevated (166°C). Dart's data (1959) showed losses at elevated temperatures as well, but he acknowledged that due to the lack of convection in the experiment, fins and tubes are at approximately the same temperature. Dart stated that in the case of cooling in air conditioning with air flow through the fins, the effect might be completely changed. Jeong *et al.* (2006) varied the hot water inlet temperature by 30°C and found no significant effects on resistance. Sheffield *et al.* (1989) stressed the importance of contact pressure (interference) for the resistance, but did not include operating temperature as a factor in their proposed correlations.

It was found in this experiment that for a steady air inlet temperature, the resistance rose linearly with decreasing fluid inlet temperature. The air inlet temperature did not have a clear effect on the overall resistance. With the tubes cooled by the liquid and the fins heated by the air, the tubes contracted away from the fins and thereby decreased contact pressure. This trend is counter to the trends seen by Gardner and Carnavos (1960) and Dart (1959). In the first case, the direction of heat flux is from the tubes to the fins. Although convection on the air side is present here, this reversed heat flux can lead to very different results. In the latter case, air-side convection was prevented and the temperature distribution between the hot and cold tubes does not represent realistic operating conditions. For refrigeration applications with similar boundary conditions as in this present experiment, an increase in resistance can be expected with decreasing tube-side temperatures in the absence of condensation.

Since the fluid temperature had to be changed during the experiment in order to achieve frosting, this dependence on the fluid inlet temperature had to be taken into account when calculating the contact resistance. Therefore, extensive measurements were completed for different air Reynolds numbers and different fluid temperatures. To calculate the contact resistance, the overall resistance under dry conditions was extrapolated to the frosting temperature, since using any other temperature would be arbitrary.

Representative data of the temperature dependence for each of the four heat exchangers are shown in Figure 5. The parameters  $a$  and  $b$  for the temperature dependence curve fit are included in Tables 3 to 6. As expected, the resistances were highest for the lower Reynolds numbers. Each point on the figure is an average of 100+ data points obtained at the respective temperature. The uncertainties in the parameters  $a$  and  $b$  led to uncertainties of the extrapolated dry resistance of up to  $\pm 7\%$ . All heat exchangers were tested over the same range of air mass flow rates, but the difference in fin spacing led to a different range of Reynolds numbers for heat exchangers 1 and 2 (fin spacing of 394 FPM) and 3 and 4 (591 FPM). Nevertheless, for both sets it is obvious that the lack of expansion in coils 1 and 3 led to far higher overall resistances. Although the magnitude of the temperature dependence varies from one heat exchanger to the other, the trends are easily noticeable and cannot be neglected.

These variations in the resistance over a relatively small temperature range show that the operating temperature must be taken into account when reporting contact resistance, since the contact pressure at the tube-fin interface is strongly influenced by the local temperatures. This shows an inherent problem with the method proposed by Dart, which has been adopted by many researchers, where the hot and cold tubes are assumed to have the same contact resistance. This is not to say that Dart's method cannot be used for the purpose of quality assurance. Heat exchangers can be tested under identical conditions and then compared to each other, but the method or correlations derived from it do not necessarily provide an accurate representation of contact resistance under normal operating conditions where the temperature distribution in the heat exchanger is very different.

### 3.2 Contact Resistance

During the frosting part of the experiment, frost was assumed to build up first on the tubes, which are the coldest surfaces of the heat exchanger. Then frost slowly started to cover the fin surfaces, starting from the outer edges of the heat exchanger towards the inside (see Figure 6). The minimum resistance occurred shortly after the coolant reached -11°C and the humidifier was turned on. After that, the resistance rose quickly due to frost buildup on the fin surfaces. As seen in Figure 7, frost eventually blocks a large part of the heat exchanger and thereby increases its resistance.

The resistances for all four heat exchangers at different air flow rates are shown in Figure 8. The resistance under dry conditions is calculated from the temperature dependence; the minimum resistance under frosting conditions is measured directly. The contact resistance as a percentage of the overall resistance is shown in Figure 9. Only heat exchanger 1 (394 FPM, unexpanded) has a contact resistance above 50% of the total resistance. Heat exchanger 2 is between 20 and 30%, sample 3 between 30 and 40%, and sample 4 roughly between 10 and 20%, depending on air flow rates. The unexpanded heat exchangers have a much higher overall resistance than do the expanded ones, and a large fin spacing (lower fin density) also increases resistance. The absolute values of the contact resistance can be seen in Figure 8. Figure 10 provides the contact resistance for a unit contact area.

The scatter in the frosting data is due to difficulties in achieving uniform frost distribution on a repeated basis. The small scatter in the data obtained under dry conditions is exacerbated by the extrapolation to lower temperatures.

Despite the uncertainty, the data convincingly show that the flow rate of air has a small effect on the contact resistance. In general, the resistance decreases with increasing air flow rate. This effect is small, although it is clear that the presence of air-side convection is crucial in order to establish realistic boundary conditions. This leads to a temperature distribution in the fins that is very different from that in Dart's method and makes the results more applicable. It is also clear that the contact resistance is not negligible for any of the heat exchangers. If an expansion tool is worn out and the contact pressure is not as high as it is designed to be, the heat exchanger performance can suffer considerably. If the heat exchanger is used in an application where

frosting or condensation occurs, the resistance can be reduced significantly and the use of an expanded heat exchanger instead of a brazed one is justified.

### 3.3 Figures

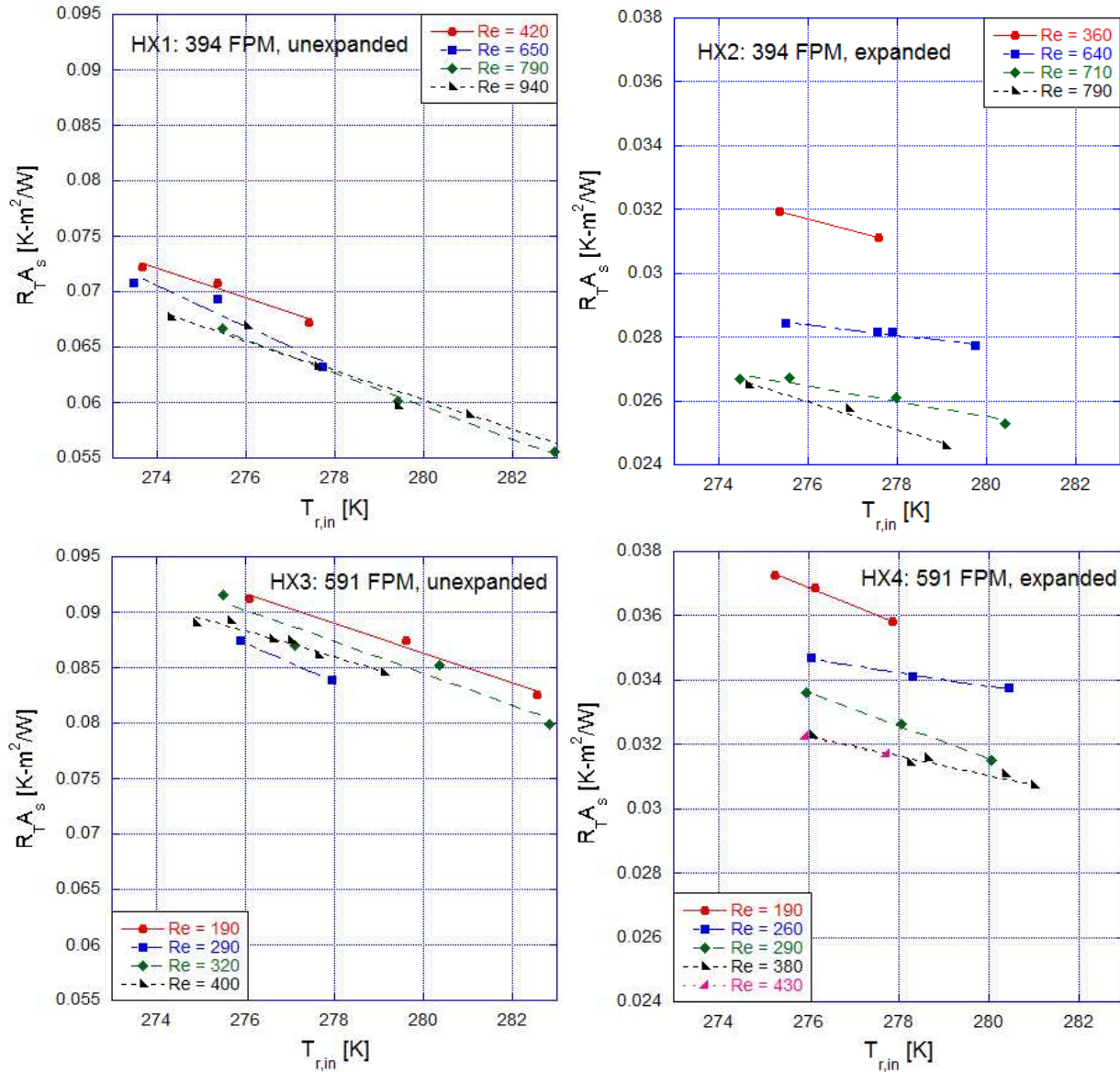


Figure 5: Temperature dependence of resistance for a unit surface area for different Reynolds numbers



Figure 6: Heat exchanger 2 at time of minimum resistance with frost starting to build up between fins at the top

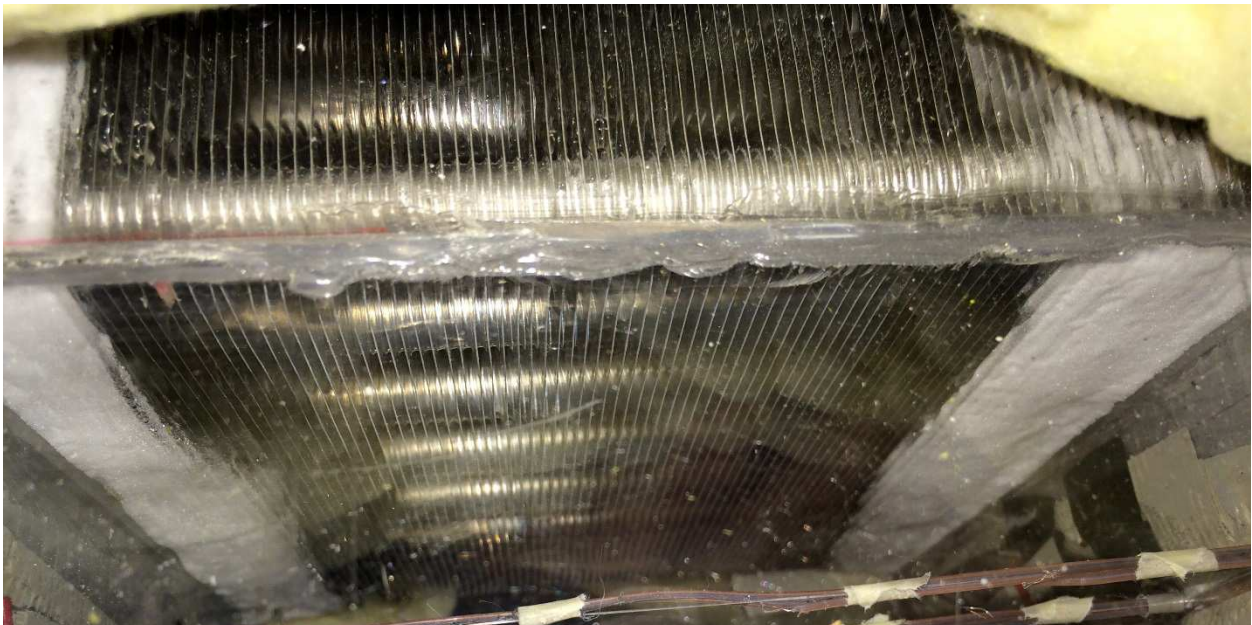


Figure 7: Heat exchanger 3 with excessive frost buildup from the sides

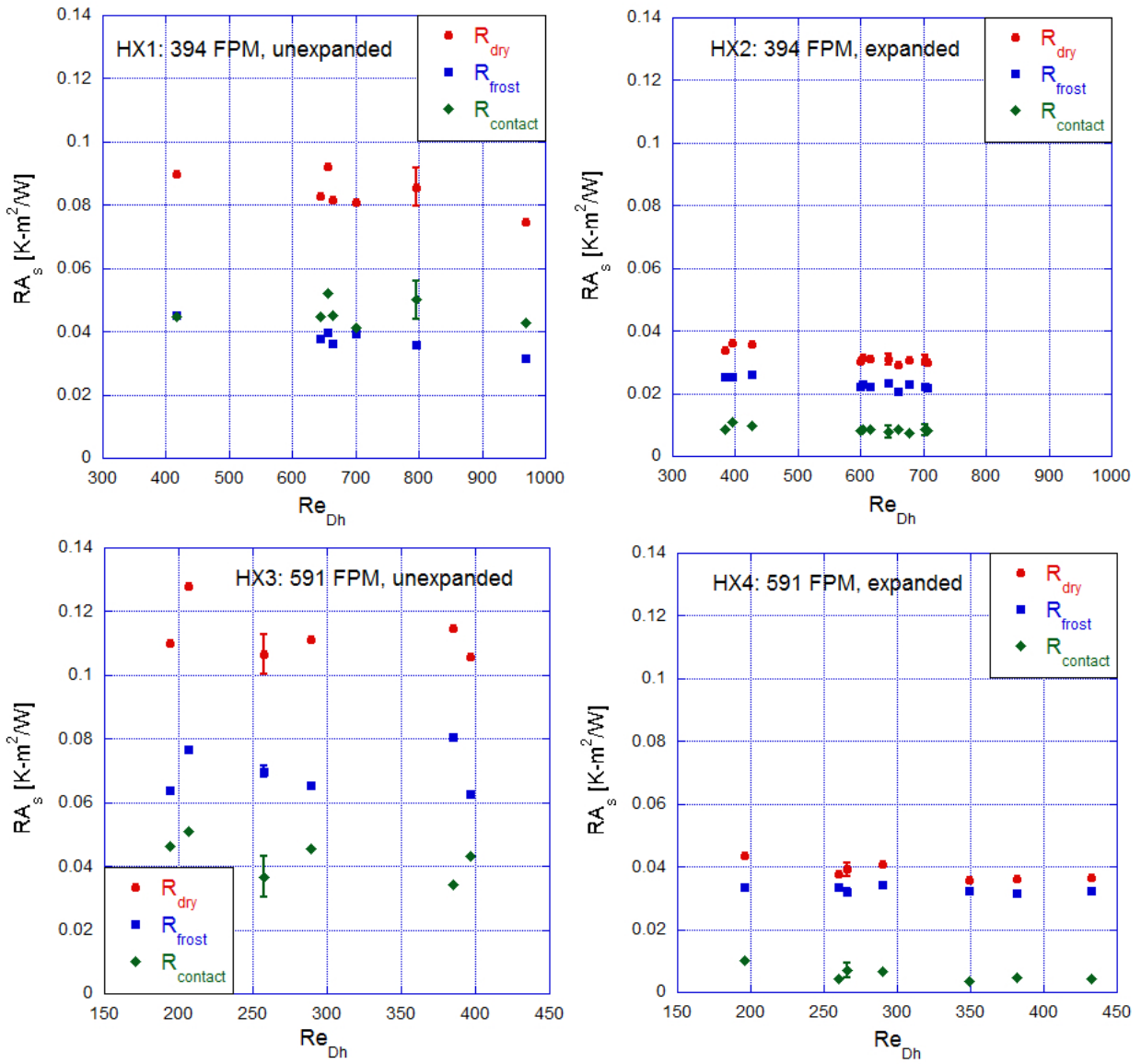


Figure 8: Resistances for unit surface area under dry and frosted conditions and calculated contact resistance

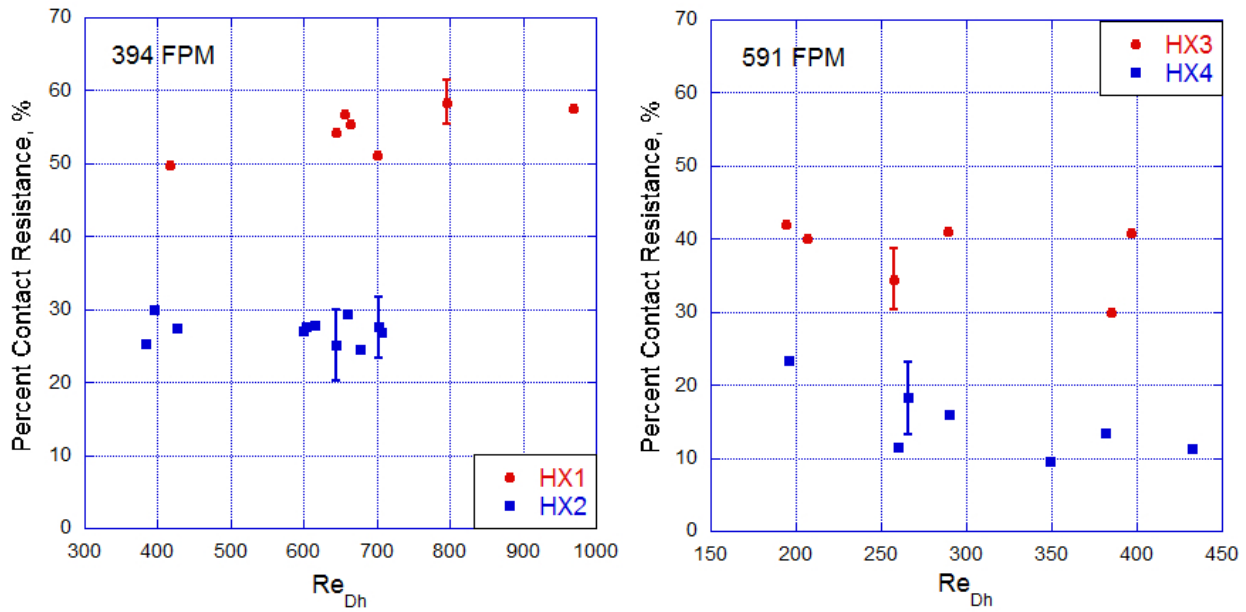


Figure 9: Contact resistance in percent of overall resistance

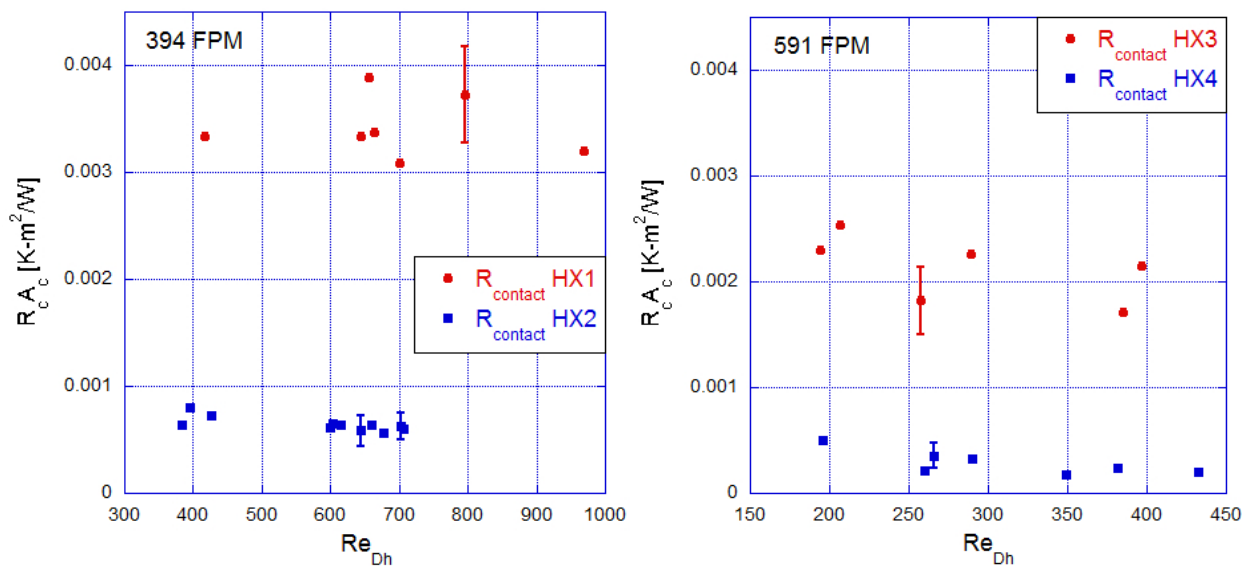


Figure 10: Contact resistance for unit contact area

### 3.4 Tables

Table 3: Heat exchanger 1: Resistances and temperature dependence parameters  $a$  and  $b$  at different Reynolds numbers

$Re_{Dh}$	$R_{dry}$	$R_{frost}$	$R_{contact}$	$R_c \%$	$a$	$b$
779	0.0816	0.0410	0.0406	49.8	-0.00135	0.436
1223	0.0835	0.0361	0.0474	56.8	-0.00166	0.519
1202	0.0750	0.0343	0.0407	54.3	-0.00086	0.299
1237	0.0741	0.0330	0.0411	55.5	-0.00173	0.526
1484	0.0778	0.0324	0.0454	58.4	-0.00133	0.428
1308	0.0734	0.0358	0.0376	51.2	-0.00087	0.302
1808	0.0677	0.0287	0.0390	57.6	-0.00065	0.239

Table 4: Heat exchanger 2: Resistances and temperature dependence parameters  $a$  and  $b$  at different Reynolds numbers

$Re_{Dh}$	$R_{dry}$	$R_{frost}$	$R_{contact}$	$R_c \%$	$a$	$b$
1230	0.0266	0.0188	0.0078	29.3	-0.000158	0.0681
1204	0.0282	0.0211	0.0071	25.2	-0.000257	0.0956
716	0.0308	0.0230	0.0078	25.3	-0.000181	0.0784
1119	0.0274	0.0200	0.0074	27.0	-0.000166	0.0709
1148	0.0281	0.0203	0.0078	27.8	-0.000216	0.0846
1312	0.0278	0.0201	0.0077	27.6	-0.000221	0.0857
736	0.0327	0.0229	0.0098	29.9	-0.000244	0.0958
795	0.0325	0.0236	0.0089	27.4	-0.000244	0.0958
1263	0.0278	0.0210	0.0068	24.5	-0.000186	0.0766
1320	0.0272	0.0199	0.0073	26.8	-0.000235	0.0888
1126	0.0287	0.0208	0.0079	27.5	-0.000258	0.0964

Table 5: Heat exchanger 3: Resistances and temperature dependence parameters  $a$  and  $b$  at different Reynolds numbers

$Re_{Dh}$	$R_{dry}$	$R_{frost}$	$R_{contact}$	$R_c \%$	$a$	$b$
760	0.0640	0.0378	0.0262	40.9	-0.00075	0.260
373	0.0665	0.0385	0.0280	42.1	-0.00079	0.273
555	0.0672	0.0396	0.0276	41.1	-0.00103	0.338
739	0.0695	0.0487	0.0208	29.9	-0.00102	0.337
396	0.0773	0.0464	0.0309	40.0	-0.00134	0.428
494	0.0644	0.0422	0.0222	34.5	-0.00042	0.174

Table 6: Heat exchanger 4: Resistances and temperature dependence parameters  $a$  and  $b$  at different Reynolds numbers

$Re_{Dh}$	$R_{dry}$	$R_{frost}$	$R_{contact}$	$R_c \%$	$a$	$b$
732	0.0219	0.0190	0.0030	13.4	-0.000175	0.0678
829	0.0221	0.0196	0.0025	11.3	-0.000186	0.0709
670	0.0217	0.0196	0.0021	9.6	-0.000086	0.0443
376	0.0264	0.0202	0.0062	23.4	-0.000251	0.0920
498	0.0228	0.0202	0.0026	11.4	-0.000130	0.0570
556	0.0247	0.0207	0.0040	16.0	-0.000309	0.1056
509	0.0237	0.0194	0.0043	18.2	-0.000220	0.0813

## Chapter 4 – Conclusion

The contact resistance of fin-and-tube heat exchangers was evaluated by conducting experiments under dry and frosted conditions. Four heat exchangers with two different values of fin spacing and contact pressures were examined. The experiments showed that contact resistance cannot be neglected when evaluating the performance of a heat exchanger. Even in the expanded heat exchangers, the contact resistance is substantial and was found to be between 10 and 30% of the overall thermal resistance. The contact resistance becomes prohibitive in the case of a faulty expansion process, which led to 30 to 60% of the total resistance.

On the other hand, the experiments showed that the presence of condensation or light frost can decrease the resistance considerably. Therefore, expanded tube heat exchangers can be suitable for cooling applications, if the contact pressure between fins and tubes is adequate. The other aspect that became clear is the importance of temperature distribution and operating conditions in order to evaluate a heat exchanger realistically. Air-side convection cannot be excluded if any statement is to be made about the actual performance of heat exchangers. Temperature distribution has to match real conditions as closely as possible in order to obtain quantitative information.

## References

- Critoph, R. E., Holland, M. K., & Turner, L. (1996). Contact resistance in air-cooled plate fin-tube air-conditioning condensers. *International Journal of Refrigeration*, 19(6), 400-406.
- Dart, D. M. (1959). Effect of fin bond on heat transfer. *ASHRAE Journal*, 1, 67-71.
- Domingos, J. D. (1969). Analysis of complex assemblies of heat exchangers. *International Journal of Heat and Mass Transfer*(12), 537-548.
- ElSherbini, A. I., Jacobi, A. M., & Hrnjak, P. S. (2003). Experimental investigation of thermal contact resistance in plain-fin-and-tube evaporators with collarless fins. *International Journal of Refrigeration*(26), 527-536.
- Ernest, T. L., Sheffield, J. W., & Sauer, H. J. (1985). Finned Tube Contact Conductance: Characterizing the Integrity of the Mechanical Bond. *Am. Soc. of Heating, Refrig. and Air-Conditioning Eng. Semiann. Meeting* (pp. 85-99). Honolulu, Hawaii: Am. Soc. of Heating, Refrig. and Air-Conditioning Eng.
- Gardner, K. A., & Carnavos, T. C. (1960). Thermal-Contact Resistance in Finned Tubing. *Journal of Heat Transfer*, 279-290.
- Incropera, F. P., Dewitt, D. P., Bergman, T. L., & Lavine, A. S. (2007). *Fundamentals of Heat and Mass Transfer* (6th ed.). Hoboken, NJ: John Wiley & Sons, Inc.
- Jeong, J., Kim, C. N., & Youn, B. (2006). A study on the thermal contact conductance in fin-tube heat exchangers with 7 mm tube. *International Journal of Heat and Mass Transfer*(49), 1547-1555.
- Jeong, J., Kim, C. N., Youn, B., & Kim, Y. S. (2004). A study on the correlation between the thermal contact conductance and effective factors in fin-tube heat exchangers with 9.52 mm tube. *International Journal of Heat and Fluid Flow*(25), 1006-1014.
- Kays, W. M., & London, A. L. (1984). *Compact Heat Exchangers* (3rd ed.). (H. B. Crawford, & D. Gleason, Eds.) USA: McGraw-Hill, Inc.

- Kim, C. N., Jeong, J., & Youn, B. (2003). Evaluation of thermal contact conductance using a new experimental-numerical method in fin-tube heat exchangers. *International Journal of Refrigeration*(26), 900-908.
- Madhusudana, C. V., Fletcher, L. S., & Peterson, G. P. (1990). Thermal Conductance of Cylindrical Joints - A Critical Review. *Journal of Thermophysics*, 4(2), 204-211.
- Park, Y.-G., Liu, L., & Jacobi, A. (2010). Rational approaches for combining redundant, independent measurements to minimize combined experimental uncertainty. *Experimental Thermal and Fluid Science*, 34, 720-724.
- Sheffield, J. W., Abu-Ebid, M., & Sauer, H. J. (1985). Finned tube contact conductance: empirical correlation of thermal conductance. *ASHRAE Trans*, 91(2a), 100-117.
- Sheffield, J. W., Stafford, B. D., & Sauer, H. (1985). Finned-Tube Contact Conductance: Investigation of Contacting Surfaces. *ASHRAE Transactions*, 91(1A), 442-452.
- Sheffield, J., Wood, R., & Sauer, H. (1989). Experimental Investigation of Thermal Conductance of Finned Tube Contacts. *Experimental Thermal and Fluid Science*, 2, 107-121.

## Appendix A – Uncertainty Analysis

An uncertainty analysis was conducted using the uncertainty propagation function in EES (Engineering Equation Solver). Individual measurement uncertainties are given in Table 7. The uncertainty for the air temperature measurement is the combined uncertainty of the upstream and downstream thermocouples, respectively. Some of the individual thermocouple measurements had a high uncertainty, so a method developed by Park et al. (2010) was employed that gives more weight to measurements with a low uncertainty. The individual uncertainties are given in Table 9 and Table 10 in Appendix C. The thermocouples upstream of the test section are # 1-5, 16-25, 38-42. Downstream are # 6-15, 26-37, 43-45. Those thermocouples not included in Table 9 and Table 10 broke during or after installation. The combined uncertainty of these thermocouples is better than any of the individual uncertainties. Weight factors are calculated from individual uncertainties with Eq. 17.

$$\Phi_i = \frac{1/u_i^2}{\sum(1/u_j^2)} \quad 17)$$

The temperature measurements are averaged according to Eq. 18 and the overall uncertainty is given by Eq. 19.

$$T = \sum \Phi_i T_i \quad 18)$$

$$u = \sqrt{\sum(\Phi_i^2 u_i^2)} \quad 19)$$

This averaging method is included in the Matlab program (Appendix C) that applies the calibration curves to the raw data. The output of the program are the averaged temperatures.

*Table 7: Measurement uncertainties*

Parameter	Uncertainty
Air temperature	$\pm 0.049^\circ\text{C}$ (US*), $\pm 0.072^\circ\text{C}$ (DS*)
Coolant temperature	$\pm 0.029^\circ\text{C}$ (US), $\pm 0.025^\circ\text{C}$ (DS)
Coolant mass flow rate	$\pm 0.01\%$ of reading
Relative humidity	$\pm 2\%$ RH
Air velocity	$\pm 5\%$ of reading or $\pm 1\%$ of full scale (20m/s)

\* US – upstream; DS - downstream

The uncertainty of the contact resistance was mainly influenced by the measurement uncertainties of the inlet and outlet temperatures of both streams and by the uncertainty of the fitting parameters for extrapolating the overall resistance to frosting temperature.

EES program:

```
//Inlet and outlet temperatures
Tc1=278.3332581[K]
Tc2=279.572999[K]
Th1=287.3560578[K]
Th2=283.7027109[K]

//Mass flow and heat capacity rates
m_dot_f=INTERPOLATE1('Lookup
2',Tc1,m_dot_f,Tc1=Tc1)
Tcm=(Tc1+Tc2)/2
cc=Interpolate('EG',Tc,specificheat,Tc=Tcm)
{specific heat fluid}
rho_h=density(Air,T=Th1,P=101325[Pa]) {air
density}
Dew=275[K]
ch=Cp(AirH2O,T=Th1,D=Dew,P=101325[Pa])
{specific heat air}

ca=ch*m_dot_a {heat capacity rate air}
cf=cc*m_dot_f {heat capacity rate fluid}
R=min(ca,cf)/max(ca,cf) {heat capacity ratio}

//Energy balance
q=ca*(Th1-Th2)
q=cf*(Tc2-Tc1)
q_max=min(ca,cf)*(Th1-Tc1)

//Effectiveness epsilon and NTU
epsilon=(Th1-Th2)/(Th1-Tc1)
ca2=ca/6 {reduced heat capacity rate for tube
passes}
Cr=min(ca2,cf)/max(ca2,cf) {reduced heat
capacity ratio}
epsilon_P=1/Cr-(Cr*exp(Cr-
(Cr/exp(NTU_P))))^-1 {effectiveness per pass}
epsilon_L=1/R*(1-(1-R*epsilon_P/6)^6)
{effectiveness per column}
epsilon=(1-(1-epsilon_L*R)/(1-
epsilon_L))^3/(R*((1-epsilon_L*R)/(1-
epsilon_L))^3) {overall effectiveness}

//Total resistance, dry and frosted
R_total=1/(NTU_P*3*ca)
a=-2.57e-4 {parameters for temperature
dependence}
b=9.56E-02
R_max=a*262+b {dry resistance}
R_min=.0211 {frosted resistance}

//Contact resistance
R_c=R_max-R_min
R_cp=R_c/R_max*100 {contact resistance % of
total resistance}
```

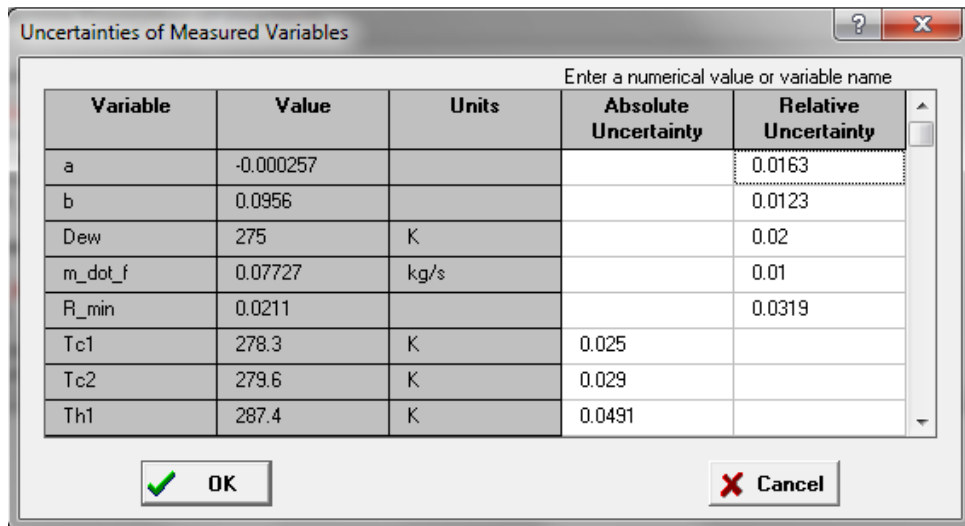


Figure 11: Uncertainties of Measured Variables in EES Uncertainty Propagation

Results from uncertainty propagation:

Variable±Uncertainty	Partial derivative	% of uncertainty
$\varepsilon = 0.4049 \pm 0.008664$		
$a = -0.000257 \pm 0.000004189$	$\partial \varepsilon / \partial a = 0$	0.00 %
$b = 0.0956 \pm 0.001176$	$\partial \varepsilon / \partial b = 0$	0.00 %
$Dew = 275 \pm 5.5 [K]$	$\partial \varepsilon / \partial Dew = 0$	0.00 %
$\dot{m}_f = 0.07735 \pm 0.0007735 [kg/s]$	$\partial \varepsilon / \partial \dot{m}_f = 0$	0.00 %
$R_{min} = 0.0211 \pm 0.0006731$	$\partial \varepsilon / \partial R_{min} = 0$	0.00 %
$Tc1 = 278.3 \pm 0.025 [K]$	$\partial \varepsilon / \partial Tc1 = 0.04488$	1.68 %
$Tc2 = 279.6 \pm 0.029 [K]$	$\partial \varepsilon / \partial Tc2 = 0$	0.00 %
$Th1 = 287.4 \pm 0.0491 [K]$	$\partial \varepsilon / \partial Th1 = 0.06596$	13.97 %
$Th2 = 283.7 \pm 0.0718 [K]$	$\partial \varepsilon / \partial Th2 = -0.1108$	84.35 %
 $q = 272.1 \pm 8.835 [J/s]$		
$a = -0.000257 \pm 0.000004189$	$\partial q / \partial a = 0$	0.00 %
$b = 0.0956 \pm 0.001176$	$\partial q / \partial b = 0$	0.00 %
$Dew = 275 \pm 5.5 [K]$	$\partial q / \partial Dew = 0$	0.00 %
$\dot{m}_f = 0.07735 \pm 0.0007735 [kg/s]$	$\partial q / \partial \dot{m}_f = 3518$	9.49 %
$R_{min} = 0.0211 \pm 0.0006731$	$\partial q / \partial R_{min} = 0$	0.00 %
$Tc1 = 278.3 \pm 0.025 [K]$	$\partial q / \partial Tc1 = -219.3$	38.50 %
$Tc2 = 279.6 \pm 0.029 [K]$	$\partial q / \partial Tc2 = 219.7$	52.02 %
$Th1 = 287.4 \pm 0.0491 [K]$	$\partial q / \partial Th1 = 0$	0.00 %
$Th2 = 283.7 \pm 0.0718 [K]$	$\partial q / \partial Th2 = 0$	0.00 %
 $R_c = 0.007166 \pm 0.001744$		
$a = -0.000257 \pm 0.000004189$	$\partial R_c / \partial a = 262$	39.62 %
$b = 0.0956 \pm 0.001176$	$\partial R_c / \partial b = 1$	45.48 %
$Dew = 275 \pm 5.5 [K]$	$\partial R_c / \partial Dew = 0$	0.00 %
$\dot{m}_f = 0.07735 \pm 0.0007735 [kg/s]$	$\partial R_c / \partial \dot{m}_f = 0$	0.00 %
$R_{min} = 0.0211 \pm 0.0006731$	$\partial R_c / \partial R_{min} = -1$	14.90 %
$Tc1 = 278.3 \pm 0.025 [K]$	$\partial R_c / \partial Tc1 = 0$	0.00 %
$Tc2 = 279.6 \pm 0.029 [K]$	$\partial R_c / \partial Tc2 = 0$	0.00 %
$Th1 = 287.4 \pm 0.0491 [K]$	$\partial R_c / \partial Th1 = 0$	0.00 %
$Th2 = 283.7 \pm 0.0718 [K]$	$\partial R_c / \partial Th2 = 0$	0.00 %
 $R_{total} = 0.02385 \pm 0.000799 [KW]$		
$a = -0.000257 \pm 0.000004189$	$\partial R_{total} / \partial a = 2.440E-10$	0.00 %
$b = 0.0956 \pm 0.001176$	$\partial R_{total} / \partial b = 6.397E-16$	0.00 %
$Dew = 275 \pm 5.5 [K]$	$\partial R_{total} / \partial Dew = 1.358E-19$	0.00 %
$\dot{m}_f = 0.07735 \pm 0.0007735 [kg/s]$	$\partial R_{total} / \partial \dot{m}_f = -0.3083$	8.91 %
$R_{min} = 0.0211 \pm 0.0006731$	$\partial R_{total} / \partial R_{min} = 2.036E-15$	0.00 %
$Tc1 = 278.3 \pm 0.025 [K]$	$\partial R_{total} / \partial Tc1 = 0.01716$	28.83 %
$Tc2 = 279.6 \pm 0.029 [K]$	$\partial R_{total} / \partial Tc2 = -0.02093$	57.69 %
$Th1 = 287.4 \pm 0.0491 [K]$	$\partial R_{total} / \partial Th1 = 0.00162$	0.99 %
$Th2 = 283.7 \pm 0.0718 [K]$	$\partial R_{total} / \partial Th2 = 0.002104$	3.58 %

## Appendix B – Data Processing

The equations given in Section 2.3 are included in the EES program below. After applying the calibration curves to the raw data and averaging the temperature measurements of the thermocouples, the data is copied into EES in order to calculate the resistance. The air mass flow rate is first calculated from the energy balance and then corrected for the presence of condensation in the frosting part of the experiment. The fluid inlet and outlet temperatures ( $T_{c1}$  and  $T_{c2}$ ) and the air inlet and outlet temperatures ( $T_{h1}$  and  $T_{h2}$ ) are inserted into a Parametric Table in EES. The fluid mass flow rates that were recorded at all inlet temperatures are provided in a Lookup Table (Figure 12). The fluid properties for the aqueous ethylene glycol mixture with 68% EG are obtained from a Lookup Table as well (Figure 13). The output is transferred to Excel, where the temperature dependence, the minimum resistance, and the contact resistance are determined.

```
//fluid mass flow rate
m_dot_f=INTERPOLATE1('Lookup 2',Tc1m,m_dot_f,Tc1m=Tc1)
//specific heat of fluid
cc=Interpolate('EG',Tc,specificheat,Tc=Tcm)
//air density
rho_h=density(Air,T=Th1,P=101325[Pa])
//dew point average
Dew=282[K]
//specific heat of air
ch=Cp(AirH2O,T=Th1,D=Dew,P=101325[Pa])
//heat capacity rates
ca=ch*m_dot_a
cf=cc*m_dot_f
//ratio of heat capacity rates
R=min(ca,cf)/max(ca,cf)
//energy balance
q=ca*(Th1-Th2)
q=cf*(Tc2-Tc1)
//max heat transfer
q_max=min(ca,cf)*(Th1-Tc1)
//heat exchanger effectiveness
epsilon=q/q_max
//reduced air heat capacity rate for individual tube passes
ca2=ca/6
//reduced ratio of heat capacity rates
Cr=min(ca2,cf)/max(ca2,cf)
//effectivenesses of passes, columns, and overall
epsilon_P=1/Cr-(Cr*exp(Cr-(Cr/exp(NTU_P))))^(-1)
epsilon_L=1/R*(1-(1-R*epsilon_P/6)^6)
epsilon=(1-((1-epsilon_L*R)/(1-epsilon_L))^3)/(R-((1-epsilon_L*R)/(1-epsilon_L))^3)
//total resistance to heat transfer
R_total=1/(NTU_P*3*ca)
```

	<input type="button" value="&lt;&gt;&gt;"/> 1	Tc1m [K]	<input type="button" value="&gt;"/> 2	m <sub>f</sub> [kg/s]	<input type="button" value="&gt;"/>
Row 1		283.2		0.07808	
Row 2		280.4		0.07766	
Row 3		277.6		0.07724	
Row 4		262.2		0.07496	

Figure 12: Lookup Table for fluid mass flow rate

	<input type="button" value="&lt;&gt;&gt;"/> 1	Tc [K]	<input type="button" value="&gt;"/> 2	density [kg/m <sup>3</sup> ]	<input type="button" value="&gt;"/> 3	specificeat [J/kg-K]	<input type="button" value="&gt;"/>
Row 1		258.2		1111		2738	
Row 2		263.2		1110		2762	
Row 3		268.2		1108		2786	
Row 4		273.2		1106		2810	
Row 5		278.2		1104		2834	
Row 6		283.2		1102		2858	
Row 7		288.2		1099		2881	
Row 8		293.2		1097		2905	
Row 9		298.2		1094		2930	
Row 10		303.2		1092		2953	
Row 11		308.2		1089		2977	

Figure 13: Lookup Table for fluid properties

## Appendix C – Calibrations

RTD calibration curves:

$$T = a * RTD + b$$

RTD 1 measured the coolant outlet temperature, RTD 4 the inlet temperature. RTD 2 was used to monitor the ambient temperature. RTD 3 was a backup. The calibration was carried out with 80 data points.

*Table 8: Calibration curves and uncertainty for RTDs*

RTD#	a	b	uncert (°C)	R <sup>2</sup>
1	5531.351	-61.961	0.025	0.999999
2	5536.750	-62.082	0.03	0.999999
3	5549.425	-62.220	0.031	0.999999
4	5540.526	-62.134	0.029	0.999999

Thermocouple calibration curves:

$$T = a * TC^2 + b * TC + c$$

Thermocouples 1-5, 16-25, and 38-42 were installed to measure the upstream air temperature. Thermocouples 6-15, 26-37, and 43-45 were downstream of the test section. The thermocouples not included in Table 9 and Table 10 broke during or after installation. The calibration was done with 20 data points.

*Table 9: Thermocouple calibration curves and uncertainties for upstream thermocouples*

TC#	a	b	c	uncert (°C)	R <sup>2</sup>
1	-5.879E+05	2.570E+04	4.180E-02	0.180	1.0000
2	-1.231E+06	2.642E+04	5.061E-01	0.630	0.9995
3	-8.009E+05	2.605E+00	4.000E+00	0.530	0.9997
5	-6.865E+05	2.597E+04	4.200E-02	0.330	0.9999
17	-8.691E+05	2.624E+04	8.881E-02	0.218	0.9999
18	-7.794E+05	2.598E+04	1.409E-01	0.239	0.9999
19	-5.894E+05	2.586E+04	6.305E-04	0.193	1.0000
20	-6.727E+05	2.594E+04	2.032E-01	0.196	1.0000
21	-8.604E+05	2.620E+04	-6.744E-03	0.268	0.9999

22	-6.475E+05	2.596E+04	-2.006E-02	0.310	0.9999
23	-8.470E+05	2.607E+04	6.447E-02	0.295	0.9999
24	-7.894E+05	2.618E+04	2.880E-01	0.216	0.9999
25	-6.284E+05	2.588E+04	-9.230E-02	0.249	0.9999
39	-8.237E+05	2.608E+04	-7.303E-02	0.253	0.9999
41	-6.707E+05	2.595E+04	-1.329E-01	0.097	1.0000
42	-7.800E+05	2.605E+04	-1.144E-01	0.111	1.0000

Table 10: Thermocouple calibration curves and uncertainties for downstream thermocouples

TC#	a	b	c	uncert (°C)	R <sup>2</sup>
6	-8.727E+05	2.596E+04	7.800E-01	0.500	0.9997
9	-9.604E+05	2.601E+04	8.896E-01	0.520	0.9997
10	-6.484E+05	2.578E+04	4.702E-01	0.550	0.9996
11	-6.705E+05	2.603E+04	-5.816E-02	0.207	1.0000
12	-8.883E+05	2.606E+04	8.745E-02	0.390	0.9998
13	-7.798E+05	2.611E+04	3.258E-02	0.227	0.9999
14	-7.502E+05	2.594E+04	1.867E-01	0.268	0.9999
15	-8.553E+05	2.593E+04	2.538E-01	0.289	0.9999
27	-7.771E+05	2.603E+04	-5.697E-02	0.226	0.9999
28	-1.024E+06	2.626E+04	1.459E-01	0.309	0.9999
29	-7.764E+05	2.605E+04	-1.193E-01	0.159	1.0000
32	-6.935E+05	2.585E+04	9.663E-02	0.406	0.9998
33	-8.117E+05	2.598E+04	7.102E-01	0.361	0.9998
34	-2.129E+05	2.514E+04	1.047E+00	1.058	0.9987
35	0.000E+00	2.495E+04	8.494E-01	1.251	0.9980
37	-8.466E+05	2.593E+04	1.306E-01	0.460	0.9998
43	-5.692E+05	2.566E+04	7.605E-01	0.716	0.9994
44	-6.445E+05	2.570E+04	3.377E-01	0.342	0.9999
45	-4.295E+05	2.538E+04	3.459E-01	0.479	0.9997

The calibration data for the four RTDs is shown in Table 11. The data are the averages for each calibration temperature.

Table 11: Calibration data for RTDs

T (°C)	1	2	3	4
23.580	0.01547	0.01547	0.01546	0.01547
21.545	0.01509	0.01511	0.01509	0.01510
19.536	0.01474	0.01475	0.01474	0.01474
17.543	0.01438	0.01439	0.01438	0.01439
15.556	0.01402	0.01403	0.01402	0.01403

13.554	0.01365	0.01367	0.01366	0.01367
11.575	0.01330	0.01331	0.01331	0.01331
9.624	0.01295	0.01296	0.01296	0.01296
7.658	0.01259	0.01261	0.01260	0.01260
5.729	0.01224	0.01225	0.01224	0.01225
3.720	0.01188	0.01189	0.01188	0.01188
1.703	0.01151	0.01153	0.01152	0.01152

-0.283	0.01115	0.01116	0.01116	0.01116		27.665	0.01620	0.01620	0.01619	0.01621
-0.277	0.01115	0.01118	0.01118	0.01116		24.719	0.01567	0.01567	0.01566	0.01567
-2.275	0.01079	0.01082	0.01082	0.01080		22.672	0.01530	0.01530	0.01529	0.01531
-4.231	0.01044	0.01046	0.01046	0.01044		19.630	0.01475	0.01475	0.01474	0.01476
-6.178	0.01009	0.01010	0.01010	0.01009		17.646	0.01439	0.01440	0.01439	0.01440
-8.143	0.00973	0.00974	0.00975	0.00973		15.658	0.01403	0.01404	0.01403	0.01404
-10.122	0.00937	0.00939	0.00939	0.00936		13.641	0.01367	0.01368	0.01367	0.01368
-12.056	0.00902	0.00903	0.00903	0.00902		11.623	0.01330	0.01331	0.01330	0.01331
-14.010	0.00866	0.00868	0.00867	0.00869		9.632	0.01295	0.01296	0.01295	0.01295
-16.015	0.00830	0.00832	0.00832	0.00833		7.678	0.01260	0.01261	0.01260	0.01260
-17.927	0.00796	0.00795	0.00795	0.00798		5.673	0.01223	0.01223	0.01222	0.01224
-17.927	0.00796	0.00795	0.00795	0.00798		3.687	0.01187	0.01188	0.01188	0.01188
-16.004	0.00830	0.00831	0.00832	0.00833		-10.153	0.00936	0.00937	0.00937	0.00938
-14.044	0.00866	0.00868	0.00867	0.00869		-6.229	0.01007	0.01008	0.01008	0.01009
-12.057	0.00902	0.00902	0.00901	0.00903		-2.238	0.01080	0.01080	0.01080	0.01081
-10.131	0.00937	0.00937	0.00937	0.00937		1.713	0.01151	0.01152	0.01152	0.01153
-8.234	0.00972	0.00974	0.00974	0.00973		5.669	0.01223	0.01224	0.01224	0.01224
-6.208	0.01008	0.01010	0.01010	0.01009		9.641	0.01295	0.01296	0.01296	0.01296
-3.234	0.01062	0.01063	0.01063	0.01063		13.622	0.01367	0.01368	0.01368	0.01368
-0.254	0.01116	0.01117	0.01117	0.01117		17.661	0.01440	0.01440	0.01440	0.01441
2.722	0.01169	0.01171	0.01170	0.01171		21.696	0.01512	0.01513	0.01512	0.01513
5.701	0.01224	0.01225	0.01225	0.01224		29.693	0.01656	0.01657	0.01656	0.01657
8.679	0.01277	0.01278	0.01278	0.01278		27.564	0.01619	0.01619	0.01618	0.01619
11.635	0.01330	0.01331	0.01331	0.01331		25.686	0.01593	0.01594	0.01593	0.01594
14.586	0.01384	0.01385	0.01384	0.01385		23.630	0.01547	0.01547	0.01546	0.01548
17.590	0.01438	0.01439	0.01438	0.01439		19.635	0.01475	0.01476	0.01475	0.01476
17.594	0.01438	0.01440	0.01439	0.01439		15.597	0.01403	0.01403	0.01403	0.01404
20.617	0.01493	0.01494	0.01493	0.01494		11.614	0.01331	0.01332	0.01331	0.01332
23.677	0.01548	0.01549	0.01548	0.01549		7.660	0.01259	0.01261	0.01260	0.01261
25.662	0.01583	0.01584	0.01583	0.01584		3.691	0.01187	0.01189	0.01188	0.01189
27.686	0.01620	0.01621	0.01619	0.01620		-0.272	0.01115	0.01116	0.01116	0.01117
29.682	0.01657	0.01657	0.01655	0.01656		-4.243	0.01043	0.01044	0.01045	0.01045
27.684	0.01621	0.01621	0.01619	0.01620		-8.210	0.00971	0.00972	0.00972	0.00973
26.691	0.01602	0.01603	0.01601	0.01603		-10.153	0.00936	0.00938	0.00938	0.00938
24.713	0.01566	0.01567	0.01565	0.01567						
29.695	0.01656	0.01657	0.01655	0.01657						

The calibration data for the 45 thermocouples is shown in Table 12. They are again the averages for each calibration temperature.

Table 12: Thermocouple calibration data

T (°C)	1	2	3	4	5	6	7	8	9	10
-10.156	-0.00039	-0.00038	-0.00038	-0.00038	-0.00038	-0.0004	-0.0004	-0.0004	-0.00041	-0.00039
-6.235	-0.00024	-0.00024	-0.00024	-0.00025	-0.00024	-0.00026	-0.00026	-0.00026	-0.00027	-0.00025
-2.240	-8.60E-05	-9.05E-05	-8.42E-05	-9.07E-05	-8.24E-05	-0.00011	-9.54E-05	-0.0001	-0.00011	-9.40E-05
1.709	6.58E-05	4.56E-05	6.28E-05	5.02E-05	6.73E-05	4.09E-05	5.37E-05	4.48E-05	3.48E-05	5.69E-05
5.663	0.00022	0.000195	0.000215	0.000203	0.00022	0.000196	0.000207	0.000201	0.00019	0.000211
9.637	0.000377	0.000352	0.00037	0.000359	0.000376	0.000353	0.000364	0.000358	0.00035	0.000368
13.615	0.000536	0.00051	0.000526	0.000517	0.000533	0.000511	0.000522	0.000516	0.000507	0.000526
17.659	0.000697	0.000676	0.000688	0.000681	0.000694	0.000668	0.000691	0.000673	0.000667	0.000686
21.696	0.000861	0.00085	0.000853	0.00085	0.000858	0.000833	0.000846	0.000837	0.000832	0.000844
25.686	0.001042	0.001025	0.001031	0.001024	0.001035	0.001014	0.001024	0.001019	0.00101	0.001021
29.693	0.001186	0.001156	0.001169	0.001159	0.001178	0.001152	0.001166	0.001157	0.00115	0.001164
27.564	0.001099	0.001068	0.001081	0.001071	0.001091	0.001065	0.001078	0.00107	0.001063	0.00108
23.628	0.000937	0.000905	0.000916	0.000908	0.000928	0.000899	0.000911	0.000904	0.000895	0.000909
19.631	0.000773	0.000743	0.000753	0.000744	0.000764	0.000735	0.000746	0.00074	0.000731	0.000746
15.593	0.000612	0.000584	0.000592	0.000583	0.000603	0.000574	0.000584	0.00058	0.00057	0.000584
11.613	0.000455	0.000428	0.000442	0.000435	0.00045	0.000419	0.000434	0.000423	0.000415	0.000431
7.655	0.000299	0.000273	0.000286	0.000278	0.000294	0.000262	0.000276	0.000266	0.000259	0.000274
3.685	0.000141	0.000115	0.000129	0.00012	0.000137	0.000105	0.000118	0.000108	0.000101	0.000116
-0.278	-1.44E-05	-4.00E-05	-2.58E-05	-3.45E-05	-1.74E-05	-5.00E-05	-3.84E-05	-4.71E-05	-5.57E-05	-3.90E-05
-4.249	-0.00017	-0.00019	-0.00018	-0.00019	-0.00017	-0.0002	-0.00019	-0.0002	-0.00021	-0.00019
-8.209	-0.00032	-0.00032	-0.00032	-0.00032	-0.00032	-0.00034	-0.00014	-0.00034	-0.00034	-0.00034
-10.153	-0.0004	-0.00041	-0.00041	-0.00041	-0.0004	-0.00043	-0.00023	-0.00042	-0.00043	-0.00042

Table 12: Thermocouple calibration data, continued

<b>12</b>	<b>13</b>	<b>14</b>	<b>15</b>	<b>16</b>	<b>17</b>	<b>18</b>	<b>19</b>	<b>20</b>	<b>21</b>	<b>22</b>	<b>23</b>
-0.00038	-0.00038	-0.00039	-0.00039	-0.00039	-0.00038	-0.00039	-0.00038	-0.00038	-0.00038	-0.00038	-0.00038
-0.00024	-0.00024	-0.00024	-0.00024	-0.00026	-0.00024	-0.00025	-0.00024	-0.00025	-0.00023	-0.00024	-0.00024
-8.25E-05	-8.30E-05	-8.92E-05	-9.04E-05	-9.70E-05	-8.51E-05	-9.15E-05	-8.61E-05	-8.96E-05	-8.11E-05	-8.12E-05	-8.42E-05
6.78E-05	6.63E-05	6.22E-05	5.88E-05	4.67E-05	6.22E-05	5.58E-05	6.58E-05	5.72E-05	6.60E-05	6.87E-05	6.31E-05
0.00022	0.000218	0.000215	0.000212	0.000203	0.000212	0.000212	0.000221	0.000212	0.000217	0.000222	0.000217
0.000375	0.000373	0.000371	0.000368	0.000361	0.000367	0.00037	0.000378	0.000368	0.000372	0.000378	0.000374
0.000532	0.00053	0.000528	0.000526	0.000519	0.000525	0.000528	0.000535	0.000526	0.00053	0.000536	0.000531
0.000692	0.00069	0.000689	0.000687	0.000678	0.000682	0.000684	0.000692	0.000684	0.000692	0.000697	0.000693
0.000857	0.000856	0.000854	0.000856	0.000849	0.00085	0.000857	0.000859	0.000849	0.000862	0.000861	0.000862
0.001035	0.001034	0.001032	0.001031	0.00103	0.00103	0.001038	0.001039	0.001031	0.00104	0.001039	0.001035
0.001179	0.001177	0.001177	0.001179	0.001171	0.001171	0.001178	0.00118	0.001172	0.001178	0.001178	0.00118
0.001093	0.001091	0.00109	0.001091	0.001086	0.001087	0.001092	0.001094	0.001087	0.001091	0.001092	0.001094
0.000928	0.000928	0.000925	0.000927	0.000923	0.000926	0.00093	0.000931	0.000924	0.000928	0.000928	0.000927
0.000762	0.000765	0.000761	0.000762	0.000761	0.000764	0.000766	0.000769	0.000762	0.000766	0.000767	0.000765
0.000601	0.000605	0.000601	0.0006	0.000601	0.000604	0.000607	0.00061	0.000603	0.000607	0.000608	0.000605
0.000448	0.000451	0.000446	0.000445	0.000446	0.000449	0.000451	0.000455	0.000446	0.000453	0.000453	0.000451
0.000292	0.000295	0.00029	0.000288	0.00029	0.000293	0.000294	0.000299	0.00029	0.000297	0.000297	0.000294
0.000134	0.000138	0.000131	0.000129	0.000133	0.000136	0.000137	0.000142	0.000132	0.000139	0.000139	0.000136
-2.08E-05	-1.74E-05	-2.37E-05	-2.62E-05	-2.26E-05	-1.81E-05	-1.71E-05	-1.41E-05	-2.23E-05	-1.60E-05	-1.73E-05	-1.96E-05
-0.00017	-0.00017	-0.00017	-0.00018	-0.00017	-0.00017	-0.00017	-0.00016	-0.00017	-0.00016	-0.00017	-0.00017
-0.00032	-0.00031	-0.00032	-0.00032	-0.00031	-0.00031	-0.00031	-0.00032	-0.00032	-0.00031	-0.00031	-0.00031
-0.0004	-0.00039	-0.0004	-0.0004	-0.0004	-0.0004	-0.00039	-0.00039	-0.0004	-0.00039	-0.00039	-0.00039

Table 12: Thermocouple calibration data, continued

<b>24</b>	<b>25</b>	<b>26</b>	<b>27</b>	<b>28</b>	<b>29</b>	<b>30</b>	<b>31</b>	<b>32</b>	<b>33</b>	<b>34</b>
-0.00039	-0.00038	0.078125	-0.00038	-0.00038	-0.00038	-0.00133	-0.00039	-0.00039	-0.0004	-0.0004
-0.00025	-0.00023	0.078125	-0.00024	-0.00024	-0.00023	-0.00118	-0.00024	-0.00024	-0.00026	-0.00027
-9.32E-05	-8.01E-05	0.078125	-8.17E-05	-8.59E-05	-8.18E-05	-0.00102	-8.38E-05	-8.42E-05	-0.0001	-0.0001
4.99E-05	7.12E-05	0.078125	6.84E-05	5.84E-05	6.95E-05	-0.00087	6.85E-05	6.82E-05	4.11E-05	4.26E-05
0.000203	0.000226	0.078125	0.000223	0.000211	0.000224	-0.00071	0.000223	0.000221	0.000194	0.000197
0.000359	0.000383	0.078125	0.000379	0.000368	0.000379	-0.00055	0.000381	0.000377	0.000354	0.000354
0.000517	0.00054	0.078125	0.000536	0.000524	0.000537	-0.00039	0.000538	0.000536	0.00051	0.000513
0.000678	0.0007	0.078125	0.000698	0.000689	0.000698	0.027592	0.000699	0.000694	0.000672	0.000674
0.000841	0.000864	0.078125	0.000861	0.000859	0.00086	0.078125	0.000853	0.000857	0.00083	0.00083
0.000993	0.001006	0.078125	0.001042	0.001039	0.001044	0.075029	0.001032	0.001037	0.000996	0.001008
0.001164	0.001186	0.078125	0.001184	0.001178	0.001185	0.07709	0.001171	0.001182	0.001157	0.001149
0.001079	0.0011	0.078125	0.001098	0.001091	0.0011	0.069569	0.001085	0.001094	0.001068	0.001061
0.000918	0.000935	0.078125	0.000932	0.000923	0.000936	0.077706	0.00092	0.000928	0.000903	0.000894
0.000757	0.000773	0.078125	0.000771	0.000762	0.000775	0.073192	0.000758	0.000763	0.000741	0.000732
0.000596	0.000612	0.078125	0.00061	0.000601	0.000614	-0.00032	0.000596	0.000602	0.000578	0.000566
0.000443	0.000457	0.078125	0.000456	0.000447	0.000458	0.072455	0.000443	0.000447	0.000426	0.000412
0.000288	0.000301	0.078125	0.000298	0.00029	0.000302	0.078125	0.000286	0.000292	0.000266	0.000252
0.00013	0.000143	0.078125	0.000141	0.000133	0.000146	0.078125	0.00013	0.000135	0.000108	8.66E-05
-2.45E-05	-1.31E-05	0.078125	-1.48E-05	-2.21E-05	-8.03E-06	0.078125	-2.61E-05	-1.89E-05	-4.74E-05	-7.46E-05
-0.00017	-0.00016	0.078125	-0.00016	-0.00017	-0.00016	0.078125	-0.00018	-0.00017	-0.0002	-0.00023
-0.00032	-0.00031	0.078125	-0.00031	-0.00031	-0.00031	-0.00123	-0.00033	-0.00032	-0.00034	-0.00038
-0.0004	-0.00039	0.078125	-0.00039	-0.00039	-0.00039	-0.00131	-0.0004	-0.00041	-0.00042	-0.00047

Table 12: Thermocouple calibration data, concluded

<b>35</b>	<b>36</b>	<b>37</b>	<b>38</b>	<b>39</b>	<b>40</b>	<b>41</b>	<b>42</b>	<b>43</b>	<b>44</b>	<b>45</b>
-0.0004	0.000907	-0.00038	-0.00038	-0.00038	-0.00038	-0.00038	-0.00038	-0.0004	-0.0004	-0.00039
-0.00025	0.000912	-0.00024	-0.00023	-0.00023	-0.00023	-0.00023	-0.00023	-0.00026	-0.00025	-0.00025
-9.75E-05	0.000948	-8.27E-05	-7.94E-05	-7.91E-05	-7.95E-05	-8.12E-05	-8.26E-05	-9.92E-05	-9.54E-05	-9.32E-05
5.69E-05	0.00095	6.80E-05	7.27E-05	7.23E-05	7.28E-05	7.12E-05	6.79E-05	4.77E-05	5.68E-05	6.05E-05
0.000213	0.000953	0.000222	0.000225	0.000224	0.000226	0.000225	0.000222	0.000201	0.000211	0.000216
0.00037	0.000953	0.000378	0.000382	0.000381	0.000382	0.000381	0.00038	0.000359	0.000371	0.000373
0.000529	0.000953	0.000535	0.000539	0.000538	0.00054	0.000539	0.000538	0.000515	0.00053	0.000532
0.000688	0.000849	0.000694	0.000699	0.000698	0.0007	0.000699	0.000696	0.000674	0.000688	0.000692
0.000826	0.000955	0.000858	0.000858	0.000859	0.000862	0.00086	0.00086	0.000834	0.000849	0.00085
0.001014	0.001003	0.001035	0.001039	0.001038	0.001038	0.001034	0.001035	0.001012	0.00103	0.001032
0.001155	0.000981	0.001181	0.001183	0.001184	0.001187	0.001185	0.001184	0.001154	0.001175	0.001177
0.001066	0.000984	0.001095	0.001097	0.001098	0.001101	0.0011	0.001099	0.001066	0.001088	0.001091
0.000905	0.000976	0.000928	0.000932	0.000932	0.000939	0.000937	0.000937	0.000901	0.000924	0.000927
0.000744	0.000974	0.000764	0.00077	0.00077	0.000778	0.000776	0.000776	0.000738	0.00076	0.000764
0.000577	0.000971	0.000602	0.000609	0.000609	0.000618	0.000616	0.000615	0.000575	0.000597	0.000602
0.000414	0.00086	0.000446	0.000455	0.000453	0.00046	0.000458	0.000457	0.000421	0.000441	0.000442
0.000255	0.000327	0.000291	0.000297	0.000297	0.000304	0.000303	0.000302	0.000262	0.000284	0.000285
8.59E-05	0.000107	0.000131	0.00014	0.00014	0.000148	0.000147	0.000145	0.000102	0.000126	0.000126
-7.61E-05	-5.49E-05	-2.79E-05	-1.38E-05	-1.35E-05	-6.24E-06	-8.08E-06	-7.90E-06	-5.39E-05	-2.86E-05	-3.19E-05
-0.00023	-0.00021	-0.00018	-0.00016	-0.00016	-0.00016	-0.00016	-0.00016	-0.00021	-0.00018	-0.00019
-0.00039	0.000911	-0.00032	-0.00031	-0.00031	-0.00031	-0.00031	-0.00031	-0.00036	-0.00034	-0.00035
-0.00046	0.000919	-0.0004	-0.00038	-0.00038	-0.00038	-0.00038	-0.00038	-0.00044	-0.00041	-0.00042

The following Matlab script calculates the combined uncertainties of the thermocouples and provides the weighting factors  $\Phi$  to be used in the next script that processes and averages data from experiments.

```
function uncert(u)
% u is a vector with the individual uncertainties of a measurement
i=1;
b=length(u);
for i=1:b
    uj=0;
    for j=1:b
        uj=uj+1/(u(j))^2;
    end
    %weighting factors phi
    phi(i)=1/(u(i))^2/uj;
    combuncerta(i)=(phi(i))^2*(u(i))^2;
end
%combined uncertainty
combuncert=sqrt(sum(combuncerta))
save phi
end
```

The following Matlab script applies the calibration curves to the raw data and averages the air temperature measurements using the weighting coefficients that were previously calculated. The processed data is then stored in an excel file for further processing with the EES program shown in Appendix B.

```
function applycalibrations(data,n)
%load calibration data
load('calib.mat')
load('RTD_calib.mat')
%build matrix with calibration
coefficients
c(1,1)=TC1.p1;
c(2,1)=TC1.p2;
c(3,1)=TC1.p3;
c(1,2)=TC2.p1;
c(2,2)=TC2.p2;
c(3,2)=TC2.p3;
c(1,3)=TC3.p1;
c(2,3)=TC3.p2;
c(3,3)=TC3.p3;
c(1,4)=TC4.p1;
c(2,4)=TC4.p2;
c(3,4)=TC4.p3;
c(1,5)=TC5.p1;
c(2,5)=TC5.p2;
c(3,5)=TC5.p3;
c(1,6)=TC6.p1;
c(2,6)=TC6.p2;
c(3,6)=TC6.p3;
c(1,7)=TC7.p1;
c(2,7)=TC7.p2;
c(3,7)=TC7.p3;
c(1,8)=TC8.p1;
c(2,8)=TC8.p2;
c(3,8)=TC8.p3;
c(1,9)=TC9.p1;
c(2,9)=TC9.p2;
c(3,9)=TC9.p3;
c(1,10)=TC10.p1;
c(2,10)=TC10.p2;
c(3,10)=TC10.p3;
c(1,11)=TC11.p1;
c(2,11)=TC11.p2;
c(3,11)=TC11.p3;
c(1,12)=TC12.p1;
c(2,12)=TC12.p2;
c(3,12)=TC12.p3;
c(1,13)=TC13.p1;
c(2,13)=TC13.p2;
c(3,13)=TC13.p3;
c(1,14)=TC14.p1;
```

```

c(2,14)=TC14.p2;
c(3,14)=TC14.p3;
c(1,15)=TC15.p1;
c(2,15)=TC15.p2;
c(3,15)=TC15.p3;
c(1,16)=TC16.p1;
c(2,16)=TC16.p2;
c(3,16)=TC16.p3;
c(1,17)=TC17.p1;
c(2,17)=TC17.p2;
c(3,17)=TC17.p3;
c(1,18)=TC18.p1;
c(2,18)=TC18.p2;
c(3,18)=TC18.p3;
c(1,19)=TC19.p1;
c(2,19)=TC19.p2;
c(3,19)=TC19.p3;
c(1,20)=TC20.p1;
c(2,20)=TC20.p2;
c(3,20)=TC20.p3;
c(1,21)=TC21.p1;
c(2,21)=TC21.p2;
c(3,21)=TC21.p3;
c(1,22)=TC22.p1;
c(2,22)=TC22.p2;
c(3,22)=TC22.p3;
c(1,23)=TC23.p1;
c(2,23)=TC23.p2;
c(3,23)=TC23.p3;
c(1,24)=TC24.p1;
c(2,24)=TC24.p2;
c(3,24)=TC24.p3;
c(1,25)=TC25.p1;
c(2,25)=TC25.p2;
c(3,25)=TC25.p3;
c(1,26)=TC27.p1;
c(2,26)=TC27.p2;
c(3,26)=TC27.p3;
c(1,27)=TC27.p1;
c(2,27)=TC27.p2;
c(3,27)=TC27.p3;
c(1,28)=TC28.p1;
c(2,28)=TC28.p2;
c(3,28)=TC28.p3;
c(1,29)=TC29.p1;
c(2,29)=TC29.p2;
c(3,29)=TC29.p3;
c(1,30)=TC31.p1;
c(2,30)=TC31.p2;
c(3,30)=TC31.p3;
c(1,31)=TC31.p1;
c(2,31)=TC31.p2;
c(3,31)=TC31.p3;
c(1,32)=TC32.p1;
c(2,32)=TC32.p2;
c(3,32)=TC32.p3;
c(1,33)=TC33.p1;

c(2,33)=TC33.p2;
c(3,33)=TC33.p3;
c(1,34)=TC34.p1;
c(2,34)=TC34.p2;
c(3,34)=TC34.p3;
c(1,35)=0;
c(2,35)=TC35.p1;
c(3,35)=TC35.p2;
c(1,36)=TC37.p1;
c(2,36)=TC37.p2;
c(3,36)=TC37.p3;
c(1,37)=TC37.p1;
c(2,37)=TC37.p2;
c(3,37)=TC37.p3;
c(1,38)=TC38.p1;
c(2,38)=TC38.p2;
c(3,38)=TC38.p3;
c(1,39)=TC39.p1;
c(2,39)=TC39.p2;
c(3,39)=TC39.p3;
c(1,40)=TC40.p1;
c(2,40)=TC40.p2;
c(3,40)=TC40.p3;
c(1,41)=TC41.p1;
c(2,41)=TC41.p2;
c(3,41)=TC41.p3;
c(1,42)=TC42.p1;
c(2,42)=TC42.p2;
c(3,42)=TC42.p3;
c(1,43)=TC43.p1;
c(2,43)=TC43.p2;
c(3,43)=TC43.p3;
c(1,44)=TC44.p1;
c(2,44)=TC44.p2;
c(3,44)=TC44.p3;
c(1,45)=TC45.p1;
c(2,45)=TC45.p2;
c(3,45)=TC45.p3;
c(1,46)=0;
c(2,46)=RTD_1.p1;
c(3,46)=RTD_1.p2;
c(1,47)=0;
c(2,47)=RTD_2.p1;
c(3,47)=RTD_2.p2;
c(1,48)=0;
c(2,48)=RTD_4.p1;
c(3,48)=RTD_4.p2;
i=1;
processed=ones(n,49);
%applying the calibration
coefficients from matrix c:
for i=1:48
    for j=1:n
        processed(j,i)=c(1,i)*data(j,i)^2+c
(2,i)*data(j,i)+c(3,i);
    end
end

```

```

end
    %storing the processed data for
air temperature

Th1i=[processed(:,1:3),processed(:,5),
      processed(:,17:25),processed(:,39),
      processed(:,41:42)]; 

Th2i=[processed(:,6),processed(:,9:15),
      processed(:,27:29),processed(:,31:35),
      processed(:,37),processed(:,43:45)];
    %storing the data from
defective thermocouples

Th1rest=[processed(:,4),processed(:,16),
      processed(:,38),processed(:,40)];
 

Th2rest=[processed(:,7:8),processed(:,26),
      processed(:,30:31),processed(:,36)]; 

    %individual uncertainties of
thermocouples
    i=1;
    DS=[0.5 0.52      0.55      0.207
0.39     0.227     0.268     0.289
0.226     0.309     0.159     0.536 0.406
0.361 1.058     1.251     0.46      0.716
0.342     0.479];
    US=[0.18      0.63      0.53
0.33     0.218     0.239     0.193
0.196     0.268     0.31      0.295
0.216     0.249     0.253     0.097
0.111];

    %weighting coefficients for
averaging and combined uncertainty
    phiUS=[0.0746      0.0061
0.0086     0.0222     0.0508
0.0423     0.0648     0.0629
0.0336     0.0251     0.0278
0.0518     0.0390     0.0377
0.2567     0.1960];
    phiDS=[0.0206      0.0190
0.0170     0.1202     0.0339
0.0999     0.0717     0.0617
0.1008      0.0539     0.2037
0.0179      0.0312     0.0395
0.0046      0.0033     0.0243
0.0100      0.0440     0.0224];

    %averaging air temperatures
using the weighting coefficients
for i=1:16

Th1a(:,i)=Th1i(:,i).*phiUS(i);
end
Th1b=sum(Th1a,2);
for k=1:20

Th2a(:,k)=Th2i(:,k).*phiDS(k);
end
Th2b=sum(Th2a,2);

    %conventional average for
comparison
Th1=mean(Th1i,2);
Th2=mean(Th2i,2);
%storing refrigerant
temperature
Tc2=processed(:,46);
Tc1=processed(:,48);
save processed;
save Th1i;
save Th2i;
save Th1;
save Th2;
save Tc1;
save Tc2;
save Th1b;
save Th2b;
save Th1rest;
save Th2rest;

    %assembling data to write in
excel file

data=[Tc1+273.15,Tc2+273.15,Th1b+27
3.15,Th2b+273.15];

xlswrite('velocity0310.xlsx',data)
end

```

## Appendix D – Data

The following is a sample data set from heat exchanger 4. It shows the inlet and outlet temperatures of the fluid ( $T_c$ ) and the air ( $Th$ ) and the mass flow rates of the fluid ( $m_f$ ) and air ( $m_a$ ). The mass flow rate of air is calculated from the energy balance.

*Table 13: Data set from heat exchanger 4*

Tc1	Tc2	Th1	Th2	m_f	m_a
280.4	281.9	291.6	285	0.0777	0.0500
280.4	281.9	291.6	285	0.0777	0.0500
280.4	281.9	291.7	285	0.0777	0.0498
280.4	281.9	291.7	285	0.0777	0.0497
280.4	281.9	291.7	285	0.0777	0.0501
280.4	281.9	291.6	285	0.0777	0.0500
280.4	281.9	291.7	285	0.0777	0.0498
280.4	281.9	291.6	285	0.0777	0.0502
280.4	281.9	291.7	285	0.0777	0.0500
280.4	281.9	291.7	285.1	0.0777	0.0501
280.4	281.9	291.6	285.1	0.0777	0.0502
280.4	281.9	291.6	285	0.0777	0.0499
280.4	281.9	291.7	285	0.0777	0.0498
280.4	281.9	291.7	285.1	0.0777	0.0495
280.4	281.9	291.7	285	0.0777	0.0495
280.4	281.9	291.6	285	0.0777	0.0499
280.4	281.9	291.7	285	0.0777	0.0495
280.4	281.9	291.7	285	0.0777	0.0499
280.4	281.9	291.7	285	0.0777	0.0499
280.4	281.9	291.7	285	0.0777	0.0498
280.4	281.9	291.7	285	0.0777	0.0496
280.4	281.9	291.7	285	0.0777	0.0495
280.4	281.9	291.7	285	0.0777	0.0494
280.4	281.9	291.7	285	0.0777	0.0497
280.4	281.9	291.7	285	0.0777	0.0496
280.4	281.9	291.7	285	0.0777	0.0496
280.4	281.9	291.6	285	0.0777	0.0499
280.4	281.9	291.7	285	0.0777	0.0496
280.4	281.9	291.7	285	0.0777	0.0497
280.4	281.9	291.7	285	0.0777	0.0496
280.4	281.9	291.6	285	0.0777	0.0499
280.4	281.9	291.7	285	0.0777	0.0498
280.4	281.9	291.6	285	0.0777	0.0499
280.4	281.9	291.7	285	0.0777	0.0493
280.4	281.9	291.7	285	0.0777	0.0497
280.4	281.9	291.6	285	0.0777	0.0499
280.4	281.9	291.7	285	0.0777	0.0497
280.4	281.9	291.7	285	0.0777	0.0495
280.4	281.9	291.7	285	0.0777	0.0497
280.4	281.9	291.7	285	0.0777	0.0495

280.4	281.9	291.7	285	0.0777	0.0497
280.4	281.9	291.6	285	0.0777	0.0496
280.4	281.9	291.7	285	0.0777	0.0497
280.4	281.9	291.7	285	0.0777	0.0494
280.4	281.9	291.7	285	0.0777	0.0498
280.4	281.9	291.7	285	0.0777	0.0495
280.4	281.9	291.7	285	0.0777	0.0497
280.4	281.9	291.7	285	0.0777	0.0495
280.4	281.9	291.7	285	0.0777	0.0490
280.4	281.9	291.7	285	0.0777	0.0495
280.4	281.9	291.7	285	0.0777	0.0495
280.4	281.9	291.7	285	0.0777	0.0498
280.4	281.9	291.7	285.1	0.0777	0.0493
280.4	281.9	291.7	285	0.0777	0.0494
280.4	281.9	291.6	285	0.0777	0.0497
280.4	281.9	291.7	285	0.0777	0.0496
280.4	281.9	291.7	285	0.0777	0.0496
280.4	281.9	291.7	285.1	0.0777	0.0494
280.4	281.9	291.7	285	0.0777	0.0498
280.4	281.9	291.7	285	0.0777	0.0496
280.4	281.9	291.7	285	0.0777	0.0495
280.4	281.9	291.7	285.1	0.0777	0.0494
280.4	281.9	291.7	285	0.0777	0.0498
280.4	281.9	291.7	285	0.0777	0.0495
280.4	281.9	291.7	285	0.0777	0.0496
280.4	281.9	291.7	285.1	0.0777	0.0493
280.4	281.9	291.7	285.1	0.0777	0.0493
280.4	281.9	291.7	285.1	0.0777	0.0497
280.4	281.9	291.7	285.1	0.0777	0.0493
280.4	281.9	291.7	285.1	0.0777	0.0494
280.4	281.9	291.7	285.1	0.0777	0.0496
280.4	281.9	291.6	285.1	0.0777	0.0498
280.4	281.9	291.6	285.1	0.0777	0.0498
280.4	281.9	291.7	285.1	0.0777	0.0496
280.4	281.9	291.7	285.1	0.0777	0.0498
280.4	281.9	291.7	285.1	0.0777	0.0493
280.4	281.9	291.7	285.1	0.0777	0.0493
280.4	281.9	291.7	285.1	0.0777	0.0494



278.5	280.3	291.5	283.9	0.0774	0.0488
278.5	280.3	291.5	283.9	0.0774	0.0490
278.5	280.3	291.5	283.9	0.0774	0.0491
278.5	280.3	291.5	283.9	0.0774	0.0492
278.5	280.3	291.5	283.9	0.0774	0.0489
278.5	280.3	291.5	283.9	0.0774	0.0490
278.5	280.3	291.5	283.9	0.0774	0.0492
278.5	280.3	291.5	283.9	0.0774	0.0491
278.5	280.3	291.5	283.9	0.0774	0.0492
278.5	280.3	291.5	283.9	0.0774	0.0491
278.5	280.3	291.5	283.9	0.0774	0.0490
278.5	280.3	291.5	283.9	0.0774	0.0489
278.5	280.3	291.5	283.9	0.0774	0.0492
278.5	280.3	291.5	283.9	0.0774	0.0490
278.5	280.3	291.5	283.9	0.0774	0.0491
278.5	280.3	291.5	283.9	0.0774	0.0490
278.5	280.3	291.5	283.9	0.0774	0.0491
278.5	280.3	291.5	283.9	0.0774	0.0491
278.5	280.3	291.5	283.9	0.0774	0.0490
278.6	280.3	291.5	283.9	0.0774	0.0490
278.6	280.3	291.5	283.9	0.0774	0.0490
278.6	280.3	291.5	283.9	0.0774	0.0491
278.6	280.3	291.5	283.9	0.0774	0.0490
278.6	280.3	291.5	283.9	0.0774	0.0491
278.6	280.3	291.5	283.9	0.0774	0.0491
278.6	280.3	291.5	283.9	0.0774	0.0491
278.6	280.3	291.5	283.9	0.0774	0.0490
278.6	280.3	291.5	283.9	0.0774	0.0489
278.6	280.3	291.5	283.9	0.0774	0.0489
278.6	280.3	291.5	283.9	0.0774	0.0489
278.6	280.3	291.5	283.9	0.0774	0.0490
278.6	280.3	291.5	283.9	0.0774	0.0488
278.6	280.3	291.5	283.9	0.0774	0.0491
278.6	280.3	291.5	283.9	0.0774	0.0488
278.6	280.3	291.5	283.9	0.0774	0.0489
278.6	280.3	291.5	283.9	0.0774	0.0489
278.6	280.3	291.5	283.9	0.0774	0.0488
278.6	280.3	291.5	283.9	0.0774	0.0489
278.6	280.3	291.5	283.9	0.0774	0.0489
278.6	280.3	291.5	283.9	0.0774	0.0490
278	279.8	291.4	283.5	0.0773	0.0489
278	279.8	291.4	283.5	0.0773	0.0491
278	279.8	291.5	283.5	0.0773	0.0490
278	279.8	291.5	283.5	0.0773	0.0490
278	279.8	291.4	283.5	0.0773	0.0490
278	279.8	291.5	283.5	0.0773	0.0489
278	279.8	291.5	283.5	0.0773	0.0488
278	279.8	291.4	283.5	0.0773	0.0489
278	279.8	291.5	283.5	0.0773	0.0488
278	279.8	291.4	283.5	0.0773	0.0489
278	279.8	291.5	283.5	0.0773	0.0489



















































262	266	291.4	274.1	0.0749	0.0421
262	266	291.4	274.1	0.0749	0.0420
262	266	291.4	274.1	0.0749	0.0421
262	266	291.4	274.1	0.0749	0.0421
262	266	291.4	274.1	0.0749	0.0420
262	266	291.4	274.1	0.0749	0.0421
262	266	291.4	274.1	0.0749	0.0421
262	266	291.4	274.1	0.0749	0.0420
262	266	291.4	274.1	0.0749	0.0420
262	266	291.4	274.1	0.0749	0.0419
262	266	291.4	274.1	0.0749	0.0419
262	266	291.4	274.1	0.0749	0.0419
262	266	291.4	274.1	0.0749	0.0418
262	266	291.4	274.1	0.0749	0.0419
262	266	291.4	274.1	0.0749	0.0419
262	266	291.4	274.1	0.0749	0.0419
262	266	291.4	274	0.0749	0.0418
262	266	291.4	274	0.0749	0.0418
262	266	291.4	274.1	0.0749	0.0417
262	266	291.4	274	0.0749	0.0418
262	266	291.4	274	0.0749	0.0418
262	266	291.4	274	0.0749	0.0418
262	266	291.4	274	0.0749	0.0417
262	266	291.4	274	0.0749	0.0417
262	266	291.4	274	0.0749	0.0418
262	266	291.4	274	0.0749	0.0417
262	266	291.4	274	0.0749	0.0417
262	266	291.4	274	0.0749	0.0417
262	266	291.4	274	0.0749	0.0418
262	266	291.4	274	0.0749	0.0418
262	266	291.4	274	0.0749	0.0417
262	266	291.5	274	0.0749	0.0417
262	266	291.4	274	0.0749	0.0417
262	266	291.5	274	0.0749	0.0416
262	266	291.5	274	0.0750	0.0416
262	266	291.4	274	0.0750	0.0416
262	266	291.5	274	0.0750	0.0415
262	266	291.4	274	0.0750	0.0416
262	266	291.4	274	0.0750	0.0415
262	266	291.5	274	0.0750	0.0415
262	266	291.4	274	0.0750	0.0415
262	266	291.4	274	0.0750	0.0415
262.1	266	291.4	274	0.0750	0.0415
262.1	266	291.4	274	0.0750	0.0415
262.1	266	291.4	274	0.0750	0.0414
262.1	266	291.5	274	0.0750	0.0414
262.1	266	291.5	274	0.0750	0.0415
262.1	266	291.4	274	0.0750	0.0414
262.1	266	291.5	274	0.0750	0.0414
262.1	266	291.5	274	0.0750	0.0415
262.1	266	291.5	274	0.0750	0.0415











262.3	265.9	291.6	273.9	0.0750	0.0372
262.3	265.9	291.6	273.9	0.0750	0.0373
262.3	265.9	291.6	273.9	0.0750	0.0373
262.3	265.9	291.6	273.9	0.0750	0.0371
262.3	265.9	291.6	274	0.0750	0.0375
262.3	265.9	291.6	274	0.0750	0.0373
262.3	265.9	291.6	274	0.0750	0.0373
262.3	265.9	291.6	274	0.0750	0.0373
262.3	265.9	291.6	274	0.0750	0.0373
262.3	265.9	291.6	274	0.0750	0.0375
262.2	265.9	291.6	274	0.0750	0.0375
262.2	265.9	291.6	273.9	0.0750	0.0373
262.2	265.9	291.6	274.1	0.0750	0.0376
262.2	265.9	291.6	274	0.0750	0.0374
262.2	265.9	291.6	274	0.0750	0.0375
262.2	265.9	291.6	274	0.0750	0.0375
262.2	265.9	291.6	274	0.0750	0.0375
262.2	265.9	291.6	274	0.0750	0.0374
262.2	265.9	291.6	273.9	0.0750	0.0373
262.2	265.8	291.6	274	0.0750	0.0373
262.2	265.8	291.6	274	0.0750	0.0374
262.2	265.8	291.6	274	0.0750	0.0374
262.2	265.8	291.6	274	0.0750	0.0373
262.2	265.8	291.6	274	0.0750	0.0373
262.2	265.8	291.6	274	0.0750	0.0375
262.2	265.8	291.6	274	0.0750	0.0372
262.2	265.8	291.6	274	0.0750	0.0374
262.2	265.8	291.6	274	0.0750	0.0374
262.2	265.8	291.6	274	0.0750	0.0374
262.2	265.8	291.6	274.1	0.0750	0.0375
262.2	265.8	291.6	274.1	0.0750	0.0375
262.2	265.8	291.6	274	0.0750	0.0374
262.2	265.8	291.6	274	0.0750	0.0374
262.2	265.8	291.6	274	0.0750	0.0373
262.2	265.8	291.6	274	0.0750	0.0373
262.2	265.8	291.6	274	0.0750	0.0371
262.2	265.8	291.6	274	0.0750	0.0372
262.2	265.8	291.6	274	0.0750	0.0373
262.2	265.8	291.7	274	0.0750	0.0373
262.2	265.8	291.6	274	0.0750	0.0373
262.2	265.8	291.6	274	0.0750	0.0372
262.2	265.8	291.6	274	0.0750	0.0372
262.2	265.8	291.6	274	0.0750	0.0372
262.2	265.8	291.6	274	0.0750	0.0372
262.1	265.8	291.6	274	0.0750	0.0373
262.1	265.8	291.6	274	0.0750	0.0373
262.1	265.8	291.6	274	0.0750	0.0372
262.1	265.8	291.6	274	0.0750	0.0373
262.1	265.8	291.6	274.1	0.0750	0.0375
262.1	265.8	291.6	274.1	0.0750	0.0373
262.1	265.7	291.6	274	0.0750	0.0373









262	265.4	291.8	274.6	0.0749	0.0351
262	265.4	291.8	274.6	0.0749	0.0351
262	265.4	291.8	274.6	0.0749	0.0351
262	265.4	291.8	274.6	0.0749	0.0351
262	265.4	291.8	274.5	0.0749	0.0350
262	265.4	291.8	274.6	0.0749	0.0350
262	265.4	291.8	274.5	0.0750	0.0350
262	265.4	291.8	274.6	0.0750	0.0351
262	265.4	291.8	274.6	0.0750	0.0350
262	265.4	291.8	274.6	0.0750	0.0349
262.1	265.4	291.8	274.6	0.0750	0.0349
262.1	265.4	291.8	274.6	0.0750	0.0348
262.1	265.4	291.8	274.6	0.0750	0.0348
262.1	265.4	291.8	274.6	0.0750	0.0349
262.1	265.4	291.8	274.6	0.0750	0.0348
262.1	265.4	291.8	274.6	0.0750	0.0347
262.1	265.4	291.8	274.6	0.0750	0.0347
262.1	265.4	291.9	274.6	0.0750	0.0347
262.1	265.4	291.9	274.6	0.0750	0.0346
262.1	265.4	291.9	274.6	0.0750	0.0346
262.1	265.4	291.8	274.5	0.0750	0.0346
262.1	265.4	291.9	274.5	0.0750	0.0345
262.1	265.4	291.8	274.6	0.0750	0.0346
262.1	265.4	291.8	274.6	0.0750	0.0346
262.1	265.4	291.8	274.6	0.0750	0.0347
262.1	265.4	291.8	274.5	0.0750	0.0347
262.1	265.4	291.8	274.6	0.0750	0.0346
262.1	265.4	291.8	274.5	0.0750	0.0345
262.1	265.4	291.9	274.6	0.0750	0.0346
262.1	265.4	291.8	274.6	0.0750	0.0346
262.1	265.4	291.9	274.6	0.0750	0.0346
262.1	265.4	291.8	274.6	0.0750	0.0345
262.1	265.4	291.9	274.6	0.0750	0.0345
262.1	265.4	291.9	274.6	0.0750	0.0344
262.1	265.4	291.9	274.6	0.0750	0.0344
262.1	265.4	291.9	274.6	0.0750	0.0344
262.1	265.4	291.9	274.6	0.0750	0.0343
262.2	265.4	291.9	274.6	0.0750	0.0344
262.2	265.4	291.9	274.6	0.0750	0.0343
262.2	265.4	291.8	274.6	0.0750	0.0343
262.2	265.4	291.9	274.6	0.0750	0.0343
262.2	265.4	291.8	274.6	0.0750	0.0342
262.2	265.4	291.9	274.6	0.0750	0.0342
262.2	265.4	291.9	274.6	0.0750	0.0342









262.1	265.2	292.1	274.5	0.0750	0.0316
262.1	265.2	292.1	274.5	0.0750	0.0315
262.1	265.2	292.1	274.5	0.0750	0.0316
262.1	265.2	292.1	274.5	0.0750	0.0316
262.1	265.2	292.1	274.4	0.0750	0.0315
262.1	265.2	292.1	274.5	0.0750	0.0316
262.1	265.2	292.1	274.5	0.0750	0.0316
262.1	265.2	292.1	274.5	0.0750	0.0315
262.1	265.2	292.1	274.5	0.0750	0.0315
262.1	265.2	292.1	274.5	0.0750	0.0315
262.1	265.2	292.1	274.5	0.0750	0.0314
262.1	265.2	292.1	274.5	0.0750	0.0314
262.1	265.2	292.1	274.5	0.0750	0.0314
262.1	265.2	292.1	274.5	0.0750	0.0313
262.1	265.2	292.1	274.5	0.0750	0.0313
262.1	265.2	292.1	274.5	0.0750	0.0312
262.1	265.2	292.1	274.5	0.0750	0.0313
262.1	265.2	292.1	274.5	0.0750	0.0313
262.1	265.2	292.1	274.5	0.0750	0.0313
262.1	265.2	292.1	274.5	0.0750	0.0312
262.2	265.2	292.1	274.5	0.0750	0.0312
262.2	265.2	292.1	274.5	0.0750	0.0312
262.2	265.2	292.1	274.5	0.0750	0.0310
262.2	265.2	292.1	274.5	0.0750	0.0312
262.2	265.2	292.1	274.5	0.0750	0.0312
262.2	265.2	292.1	274.5	0.0750	0.0311
262.2	265.2	292.1	274.5	0.0750	0.0311
262.2	265.2	292.1	274.5	0.0750	0.0311
262.2	265.2	292.1	274.5	0.0750	0.0310
262.2	265.3	292.1	274.5	0.0750	0.0311
262.2	265.3	292.1	274.5	0.0750	0.0310